

Functional additive models for optimizing individualized treatment rules

HYUNG G. PARK^{a*}, EVA PETKOVA^a, THADDEUS TARPEY^a, R. TODD OGDEN^b

^a *Division of Biostatistics, Department of Population Health, New York University*

^b *Department of Biostatistics, Columbia University*

Abstract

A novel functional additive model is proposed which is uniquely modified and constrained to model nonlinear interactions between a treatment indicator and a potentially large number of functional and/or scalar pretreatment covariates. The primary motivation for this approach is to optimize individualized treatment rules based on data from a randomized clinical trial. We generalize functional additive regression models by incorporating treatment-specific components into additive effect components. A structural constraint is imposed on the treatment-specific components in order to provide a class of additive models with main effects and interaction effects that are orthogonal to each other. If primary interest is in the interaction between treatment and the covariates, as is generally the case when optimizing individualized treatment rules, we can thereby circumvent the need to estimate the main effects of the covariates, obviating the need to specify their form and thus avoiding the issue of model misspecification. The methods are illustrated with data from a depression clinical trial with electroencephalogram functional data as patients' pretreatment covariates.

Keywords: Individualized treatment rules; Functional additive regression; Sparse additive models; Treatment effect-modifiers

1 Introduction

We propose a flexible functional regression approach to optimizing individualized treatment decision rules (ITRs) where the treatment has to be chosen to optimize the expected treatment outcome. We focus on the situation in which potentially large number of patient characteristics is available as pretreatment functional and/or scalar covariates. Recent advances in biomedical imaging, mass spectrometry, and high-throughput gene expression technology produce massive amounts of data on individual patients, opening up the possibility of tailoring treatments to the biosignatures of individual patients from individual-specific data ([McKeague and Qian, 2014](#)). Notably, some randomized clinical trials (e.g., [Trivedi et al., 2016](#)) are designed to discover biosignatures that characterize patient heterogeneity in treatment responses from vast amounts of patient pretreatment characteristics. In this paper, we focus on some specific types of high-dimensional pretreatment patient characteristics observed in the form of curves or images, for instance, electroencephalogram (EEG) measurements. Such data can be viewed as functional (e.g., [Ramsay and Silverman, 1997](#)) and are becoming increasingly prevalent in modern randomized clinical trials (RCTs) as pretreatment covariates.

Much work has been carried out to develop methods for optimizing ITRs using data from RCTs. Regression-based methodologies are intended to optimize ITRs by estimating treatment-specific response (e.g., [Jeng et al., 2018](#); [Lu et al., 2011](#); [Park et al., 2020b](#); [Petkova et al., 2020](#); [Qian and Murphy, 2011](#); [Shi et al., 2016](#); [Tian et al., 2014](#)) while attempting to maintain robustness with respect to model misspecification.

⁰To whom correspondence should be addressed; parkh15@nyu.edu

Machine learning approaches for optimizing ITRs are often framed as a classification problem (e.g., Zhang et al., 2012; Zhao et al., 2019), including outcome weighted learning (e.g., Song et al., 2015; Zhao et al., 2012, 2015) based on support vector machines, tree-based classification (e.g., Laber and Zhao, 2015) and adaptive boosting (Kang et al., 2014), among others. However, to date there has been relatively little research on ITRs that directly utilize pretreatment functional covariates. McKeague and Qian (2014) proposed methods for optimizing ITRs that depend upon a single pretreatment functional covariate. The flexible functional regression approach of Ciarleglio et al. (2016) is also restricted to a single pretreatment functional covariate. Ciarleglio et al. (2015) proposed a method allowing for multiple functional/scalar covariates, and extended to incorporate a simultaneous covariate selection for ITRs in Ciarleglio et al. (2018). However, both of these approaches are limited to a stringent linear model assumption on the treatment-by-covariates interaction effects that limits flexibility in optimizing ITRs and to two treatment conditions.

In this paper, we allow for nonlinear interactions between the treatment and the pretreatment functional covariates on the outcome and also for more than two treatment conditions. We incorporate a simultaneous covariate selection for ITRs through an L^1 regularization to deal with a large number of functional and/or scalar covariates. In a review by Morris (2015) on functional regression, two popular approaches to functional additive regression are the functional additive regression of Fan et al. (2015) and the functional generalized additive model of McLean et al. (2014). In this paper, we base our method on the functional additive regression model of Fan et al. (2015) that utilizes one-dimensional data-driven functional indices and the associated additive link functions. In Ciarleglio et al. (2016), nonlinear effects are presented with the functional additive regression of McLean et al. (2014). However, the approach of McLean et al. (2014) requires more parameters for estimation and is based on an L^2 penalty rather than on L^1 penalties, which is less suitable in the context of many functional covariates and when sparsity is desired. In this paper, we develop a flexible approach to optimizing ITRs that can easily impose structural constraints in modeling nonlinear heterogeneous treatment effects with functional and/or scalar pretreatment covariates.

2 Constrained functional additive models

We consider a treatment response $Y \in \mathbb{R}$, a set of p functional-valued pretreatment covariates $\mathbf{X} = (X_1, \dots, X_p)$, and q scalar-valued pretreatment covariates $\mathbf{Z} = (Z_1, \dots, Z_q) \in \mathbb{R}^q$. These pretreatment covariates (\mathbf{X}, \mathbf{Z}) are considered as potential biomarkers for optimizing ITRs. We will assume that each X_j is a square integrable random function, defined on a compact interval, say, $[0, 1]$, without loss of generality. Suppose there are L available treatment options, with treatment indicator $A \in \{1, \dots, L\}$ assigned with associated randomization probabilities (π_1, \dots, π_L) , such that $\sum_{a=1}^L \pi_a = 1$, $\pi_a > 0$, independent of (\mathbf{X}, \mathbf{Z}) .

In this context we focus on optimizing ITRs based on (\mathbf{X}, \mathbf{Z}) . For a single decision point, an ITR based on (\mathbf{X}, \mathbf{Z}) , which we denote by \mathcal{D} , maps a patient with pretreatment characteristics (\mathbf{X}, \mathbf{Z}) to one of the treatment options in $\{1, \dots, L\}$. One popular measure of the effectiveness of \mathcal{D} is the so-called “value” (V) function (Murphy, 2005), $V(\mathcal{D}) = E[E[Y|\mathbf{X}, \mathbf{Z}, A = \mathcal{D}(\mathbf{X}, \mathbf{Z})]]$, the aggregate effect of applying a given treatment regime \mathcal{D} across the population. If we assume, without loss of generality, that a larger value of Y is better, then the optimal ITR, which we denote as \mathcal{D}^{opt} , can be defined as \mathcal{D} that maximizes $V(\mathcal{D})$. Such a rule \mathcal{D}^{opt} can be shown to satisfy: $\mathcal{D}^{opt}(\mathbf{X}, \mathbf{Z}) = \arg \max_{a \in \{1, \dots, L\}} E[Y|\mathbf{X}, \mathbf{Z}, A = a]$. In particular, \mathcal{D}^{opt} does not depend on the “main” effect of the covariates (\mathbf{X}, \mathbf{Z}) and depends only on the (\mathbf{X}, \mathbf{Z}) -by- A interaction effect (Qian and Murphy, 2011) in the mean response function $E[Y|\mathbf{X}, \mathbf{Z}, A]$. However, if this mean response model inadequately represents the interaction effect, the associated ITR may perform poorly.

Thus, we will focus on modeling possibly nonlinear (\mathbf{X}, \mathbf{Z}) -by- A interaction effects, while allowing for an unspecified main effect of (\mathbf{X}, \mathbf{Z}) . We base the model on the functional additive model (FAM) of Fan et al. (2015) allowing for nonlinear (\mathbf{X}, \mathbf{Z}) -by- A interactions:

$$E[Y|\mathbf{X}, \mathbf{Z}, A] = \underbrace{\mu(\mathbf{X}, \mathbf{Z})}_{(\mathbf{x}, \mathbf{z}) \text{ “main” effect}} + \underbrace{\sum_{j=1}^p g_j(\langle X_j, \beta_j \rangle, A) + \sum_{k=1}^q h_k(Z_k, A)}_{(\mathbf{x}, \mathbf{z})\text{-by-}A \text{ interaction effect}}. \quad (1)$$

In model (S.1), the treatment a -specific (with $a \in \{1, \dots, L\}$) component functions $\{g_j(\cdot, a), j = 1, \dots, p\} \cup \{h_k(\cdot, a), k = 1, \dots, q\}$ are unspecified smooth one-dimensional (1-D) functions. Specifically, each function X_j appears as a 1-D projection $\langle X_j, \beta_j \rangle := \int_0^1 X_j(s)\beta_j(s)ds$, via the standard L^2 inner product with a coefficient function $\beta_j \in \Theta$, where Θ is the space of square integrable functions over $[0, 1]$, restricted to a unit L^2 norm for model identifiability (due to the unspecified nature of the associated functions $g_j(\cdot, a)$). The form of the function μ in (S.1) is left unspecified. For model (S.1), we assume an additive noise, $Y = E[Y|\mathbf{X}, \mathbf{Z}, A] + \epsilon$, where $\epsilon \in \mathbb{R}$ is a zero-mean noise with finite variance.

In model (S.1), to separate the nonparametric (\mathbf{X}, \mathbf{Z}) “main” effect from the additive (\mathbf{X}, \mathbf{Z}) -by- A interaction effect components, and to obtain an identifiable representation, we will constrain the $p+q$ component functions $\{g_j, j = 1, \dots, p\} \cup \{h_k, k = 1, \dots, q\}$ associated with the (\mathbf{X}, \mathbf{Z}) -by- A interaction effect to satisfy the following identifiability conditions:

$$\begin{aligned} E[g_j(\langle X_j, \beta_j \rangle, A) | X_j] &= 0 \quad (\forall \beta_j \in \Theta) \quad (j = 1, \dots, p) \quad \text{and} \\ E[h_k(Z_k, A) | Z_k] &= 0 \quad (k = 1, \dots, q) \end{aligned} \quad (2)$$

(almost surely), where the expectation is taken with respect to the distribution of A given X_j (or Z_k). Condition (S.2) implies $E[\sum_{j=1}^p g_j(\langle X_j, \beta_j \rangle, A) + \sum_{k=1}^q h_k(Z_k, A) | \mathbf{X}, \mathbf{Z}] = 0$ (almost surely), which makes not only representation (S.1) identifiable, but also the two effect components in model (S.1) orthogonal to each other. We call model (S.1) subject to the constraint (S.2), a *constrained functional additive model* (CFAM), which is the main model of the paper.

Notation. For a fixed β , let us denote the L^2 space of component functions, $g(\cdot, \cdot)$, over the random variables $(\langle X, \beta \rangle, A)$ as: $\mathcal{H}^{(\beta)} = \{g \mid E[g(\langle X, \beta \rangle, A)] = 0, \|g\| < \infty\}$, with $\|g\| = \sqrt{E[g^2(\langle X, \beta \rangle, A)]}$, where the expectation is taken with respect to the joint distribution of $(\langle X, \beta \rangle, A)$ and the inner product of the space defined as $\langle g, g' \rangle = E[g(\langle X, \beta \rangle, A)g'(\langle X, \beta \rangle, A)]$. Similarly, let us denote the L^2 space of component functions, $h(\cdot, \cdot)$, over (Z, A) as: $\mathcal{H} = \{h \mid E[h(Z, A)] = 0, \|h\| < \infty\}$ with $\|h\| = \sqrt{E[h^2(Z, A)]}$, where the expectation is with respect to the distribution of (Z, A) , and similarly defined inner product. We suppress the treatment-specific intercepts in models, by removing the treatment a -specific means from Y , and assume $E[Y|A = a] = 0$ ($a = 1, \dots, L$), i.e., the main effect of A is 0, without loss of generality.

Under the formulation (S.1) subject to the constraint (S.2), the “true” (i.e., optimal) functions, denoted as $\{g_j^*, j = 1, \dots, p\} \cup \{\beta_j^*, j = 1, \dots, p\} \cup \{h_k^*, k = 1, \dots, q\}$ that constitute the (\mathbf{X}, \mathbf{Z}) -by- A interaction effect, can be viewed as the solution to the constrained optimization:

$$\begin{aligned} \{g_j^*, \beta_j^*, h_k^*\} &= \underset{g_j \in \mathcal{H}_j^{(\beta_j)}, \beta_j \in \Theta, h_k \in \mathcal{H}_k}{\text{argmin}} \quad E \left\{ Y - \sum_{j=1}^p g_j(\langle X_j, \beta_j \rangle, A) - \sum_{k=1}^q h_k(Z_k, A) \right\}^2, \\ \text{subject to} & \quad E[g_j(\langle X_j, \beta_j \rangle, A) | X_j] = 0 \quad \forall \beta_j \in \Theta \quad (j = 1, \dots, p) \quad \text{and} \\ & \quad E[h_k(Z_k, A) | Z_k] = 0 \quad (k = 1, \dots, q). \end{aligned} \quad (3)$$

Specifically, representation (S.4) does not involve the “main” effect functional μ , due to the orthogonal representation (S.1) implied by (S.2). (See Section A.1 of Supporting Information for additional detail.) If μ in (S.1) is a complicated functional subject to model misspecification, exploiting the representation on the right-hand side of (S.4) for $\{g_j^*, j = 1, \dots, p\} \cup \{\beta_j^*, j = 1, \dots, p\} \cup \{h_k^*, k = 1, \dots, q\}$ on the left-hand side is particularly appealing, as it provides a means of estimating the interaction terms without having to specify μ , thereby avoiding any issue of possible model misspecification for μ . The function μ can also be specified similar to (S.4) and estimated separately (see Section A.6 of Supporting Information), due to orthogonality in model (S.1). In particular, estimators of $\{g_j^*, \beta_j^*, h_k^*\}$ based on optimization (S.4) can be improved in terms of efficiency if Y in (S.4) is replaced by a “residualized” response $Y - \hat{\mu}(\mathbf{X}, \mathbf{Z})$, where $\hat{\mu}$ is some estimate of μ (see also Section A.6 of Supporting Information). However, for simplicity, we will focus on the representation (S.4) with the “unresidualized” Y .

Under model (S.1), the potential treatment effect-modifying variables among $\{X_j, j = 1, \dots, p\} \cup \{Z_k, k = 1, \dots, q\}$ appear in the model, only through the interaction effect terms in (S.1) that specify and characterize

the heterogeneous treatment effects. Ravikumar et al. (2009) proposed a sparse additive model (SAM) for relevant covariate selection in a high-dimensional additive regression. As in SAM, to deal with a large $p + q$ and to achieve treatment effect-modifying variable selection, we impose sparsity on the set of component functions $\{g_j, j = 1, \dots, p\} \cup \{h_k, k = 1, \dots, q\}$ of CFAM (S.1), under the often reasonable assumption that most covariates are inconsequential as treatment effect-modifiers. This sparsity structure on the set of component functions can be usefully incorporated into the optimization-based representation (S.4) for $\{g_j^*, \beta_j^*, h_k^*\}$:

$$\begin{aligned} \{g_j^*, \beta_j^*, h_k^*\} = & \underset{g_j \in \mathcal{H}_j^{(\beta_j)}, \beta_j \in \Theta, h_k \in \mathcal{H}_k}{\operatorname{argmin}} & E \left\{ Y - \sum_{j=1}^p g_j(\langle X_j, \beta_j \rangle, A) - \sum_{k=1}^q h_k(Z_k, A) \right\}^2 + \lambda \left\{ \sum_{j=1}^p \|g_j\| + \sum_{k=1}^q \|h_k\| \right\}, \\ \text{subject to} & & E[g_j(\langle X_j, \beta_j \rangle, A) | X_j] = 0 \quad \forall \beta_j \in \Theta \quad (j = 1, \dots, p) \quad \text{and} \\ & & E[h_k(Z_k, A) | Z_k] = 0 \quad (k = 1, \dots, q), \end{aligned} \tag{4}$$

for some sparsity-inducing parameter $\lambda \geq 0$. The term $\sum_{j=1}^p \|g_j\| + \sum_{k=1}^q \|h_k\|$ in (4) behaves like an L^1 ball across different functional components $\{g_j, j = 1, \dots, p; h_k, k = 1, \dots, q\}$ to encourage functional sparsity. For example, a relatively large value of λ in (4) will result in many components to be exactly zero, thereby enforcing sparsity on the set of functions $\{g_j^*, h_k^*\}$ on the left-hand side of (4). Specifically, equation (4) can help model selection when dealing with potentially many functional/scalar pretreatment covariates.

3 Estimation

We first consider a population characterization of the algorithm for solving (4) in Section 3.1 and then a sample counterpart of the population algorithm in Section 3.2.

3.1 Population algorithm

For a set of fixed coefficient functions $\{\beta_j, j = 1, \dots, p\}$, the minimizing component function $g_j \in \mathcal{H}_j^{(\beta_j)}$ (and $h_k \in \mathcal{H}_k$) for each j (and each k) of the constrained objective function of (4) has a component-wise closed-form expression.

Theorem 1. *Given $\lambda \geq 0$ and a set of fixed single-index coefficient functions $\{\beta_j, j = 1, \dots, p\}$, the minimizing component function $g_j \in \mathcal{H}_j^{(\beta_j)}$ of the constrained objective function of (4) satisfies:*

$$g_j(\langle X_j, \beta_j \rangle, A) = \left[1 - \frac{\lambda}{\|f_j\|} \right]_+ f_j(\langle X_j, \beta_j \rangle, A) \quad (\text{almost surely}), \tag{5}$$

where the function $f_j \in \mathcal{H}_j^{(\beta_j)}$:

$$f_j(\langle X_j, \beta_j \rangle, A) := E[R_j | \langle X_j, \beta_j \rangle, A] - E[R_j | \langle X_j, \beta_j \rangle], \tag{6}$$

in which

$$R_j = Y - \sum_{j' \neq j} g_{j'}(\langle X_{j'}, \beta_{j'} \rangle, A) - \sum_{k=1}^q h_{k,A}(Z_k) \tag{7}$$

represents the j th (functional covariate's) partial residual; similarly, the minimizing component function $h_k \in \mathcal{H}_k$ of the constrained objective function of (4) satisfies:

$$h_k(Z_k, A) = \left[1 - \frac{\lambda}{\|\check{f}_k\|} \right]_+ \check{f}_k(Z_k, A) \quad (\text{almost surely}), \tag{8}$$

where the function $\check{f}_k \in \mathcal{H}_k$:

$$\check{f}_k(Z_k, A) := E[\check{R}_k | Z_k, A] - E[\check{R}_k | Z_k], \tag{9}$$

and

$$\check{R}_k = Y - \sum_{j=1}^p g_j(\langle X_j, \beta_j \rangle, A) - \sum_{k' \neq k} h_{k'}(Z_{k'}, A) \quad (10)$$

represents the k th (scalar covariate's) partial residual. (In (5) and (8), $[u]_+ = \max(0, u)$ represents the positive part of u .)

The proof of Theorem 1 is in Section A.2 of Supporting Information. Given a sparsity tuning parameter $\lambda \geq 0$, optimization (4) can be split into two iterative steps (Fan et al., 2014, 2015). First (*Step 1*), for a set of fixed single-indices $\langle X_j, \beta_j \rangle$ ($j = 1, \dots, p$), the component functions $\{g_j, j = 1, \dots, p\} \cup \{h_k, k = 1, \dots, q\}$ of the model can be found by a coordinate descent procedure that fixes $\{g_{j'}; j' \neq j\} \cup \{h_k, k = 1, \dots, q\}$ and obtains g_j by equation (5) (and that fixes $\{g_j, j = 1, \dots, p\} \cup \{h_{k'}; k' \neq k\}$ and obtains h_k by equation (8)), and then iterates through all j and k until convergence. This step (*Step 1*) amounts to fitting a SAM (Ravikumar et al., 2009) subject to the constraint (S.2). Second (*Step 2*), for a set of fixed component functions $\{g_j, j = 1, \dots, p\} \cup \{h_k, k = 1, \dots, q\}$, the j th single-index coefficient function $\beta_j \in \Theta$ can be optimized by solving, for each $j \in \{1, \dots, p\}$ separately:

$$\text{minimize}_{\beta_j \in \Theta} E \left\{ R_j - g_j(\langle X_j, \beta_j \rangle, A) \right\}^2 \quad (j = 1, \dots, p), \quad (11)$$

where the j th partial residual R_j is defined in (7). These two steps can be iterated until convergence to obtain a population solution $\{g_j^*, \beta_j^*, h_k^*\}$ on the left-hand side of (4).

To obtain a sample version of the population solution, we can insert sample estimates into the population algorithm, as in standard backfitting in estimating generalized additive models (Hastie and Tibshirani, 1999), which we describe in the next subsection.

3.2 Sample version of the population algorithm

To simplify the exposition, we only describe the optimization of $g_j(\langle X_j, \beta_j \rangle, A)$ ($j = 1, \dots, p$) associated with the functional covariates X_j ($j = 1, \dots, p$). The components $h_k(Z_k, A)$ ($k = 1, \dots, q$) associated with the scalar covariates Z_k ($k = 1, \dots, q$) in (4) are optimized in the same way, except that we do not need to perform *Step 2* of the alternating optimization procedure; i.e., when optimizing $h_k(Z_k, A)$ ($k = 1, \dots, q$), we only perform *Step 1*.

3.2.1 Step 1

First, we consider a sample version of *Step 1* of the population algorithm. Suppose we are given a set of estimates $\{\hat{\beta}_j, j = 1, \dots, p\}$ and the data-version of the j th partial residual R_j in (7): $\hat{R}_{ij} = Y_i - \sum_{j' \neq j} \hat{g}_{j'}(\langle X_{ij'}, \hat{\beta}_{j'} \rangle, A_i) - \sum_{k=1}^q \hat{h}_k(Z_{ik}, A_i)$ ($i = 1, \dots, n$), where $\hat{g}_{j'}$ represents a current estimate for $g_{j'}$ and \hat{h}_k that for h_k . For each j , we update the component function g_j in (5) in two steps: first, estimate the function f_j in (6); second, plug the estimate of f_j into $\left[1 - \frac{\lambda}{\|f_j\|}\right]_+$ in (5), to obtain the soft-thresholded estimate \hat{g}_j .

Although any linear smoothers can be utilized to obtain estimators $\{\hat{g}_j, j = 1, \dots, p\}$ (see Section A.3 of Supporting Information), we shall focus on regression spline-type estimators, which are simple and computationally efficient to implement. For each j and $\beta_j = \hat{\beta}_j$, we will represent the component function $g_j \in \mathcal{H}_j^{(\hat{\beta}_j)}$ on the right-hand side of (4) as:

$$g_j(\langle X_j, \hat{\beta}_j \rangle, a) = \Psi_j(\langle X_j, \hat{\beta}_j \rangle)^\top \theta_{j,a} \quad (a = 1, \dots, L) \quad (12)$$

for some prespecified d_j -dimensional basis $\Psi_j(\cdot)$ (e.g., cubic B -spline basis with $d_j - 4$ interior knots, evenly placed over the range (scaled to, say, $[0, 1]$) of the observed values of $\langle X_j, \hat{\beta}_j \rangle$) and a set of unknown

treatment a -specific basis coefficients $\{\boldsymbol{\theta}_{j,a} \in \mathbb{R}^{d_j}\}_{a \in \{1, \dots, L\}}$. Based on representation (12) of $g_j \in \mathcal{H}_j^{(\widehat{\beta}_j)}$ for fixed $\widehat{\beta}_j$, the constraint $E[g_j(\langle X_j, \beta_j \rangle, A) | X_j] = 0$ in (4) on g_j , for fixed $\beta_j = \widehat{\beta}_j$, can be simplified to: $E[\boldsymbol{\theta}_{j,A}] = \sum_{a=1}^L \pi_a \boldsymbol{\theta}_{j,a} = \mathbf{0}$. If we fix $\beta_j = \widehat{\beta}_j$, the constraint in (4) on the function g_j can then be succinctly written in matrix form:

$$\boldsymbol{\pi}^{(j)} \boldsymbol{\theta}_j = \mathbf{0}, \quad (13)$$

where $\boldsymbol{\theta}_j := (\boldsymbol{\theta}_{j,1}^\top, \boldsymbol{\theta}_{j,2}^\top, \dots, \boldsymbol{\theta}_{j,L}^\top)^\top \in \mathbb{R}^{d_j L}$ is the vectorized version of the basis coefficients $\{\boldsymbol{\theta}_{j,a}\}_{a \in \{1, \dots, L\}}$, and the $d_j \times d_j L$ matrix $\boldsymbol{\pi}^{(j)} := (\pi_1 \mathbf{I}_{d_j}; \pi_2 \mathbf{I}_{d_j}; \dots; \pi_L \mathbf{I}_{d_j})$ where \mathbf{I}_{d_j} is the $d_j \times d_j$ identity matrix.

Let the $n \times d_j$ matrices $\mathbf{D}_{j,a}$ ($a = 1, \dots, L$) denote the evaluation matrices of the basis $\boldsymbol{\Psi}_j(\cdot)$ on $\langle X_{ij}, \widehat{\beta}_j \rangle$ ($i = 1, \dots, n$) specific to the treatment $A = a$ ($a = 1, \dots, L$), whose i th row is the $1 \times d_j$ vector $\boldsymbol{\Psi}_j(\langle X_{ij}, \widehat{\beta}_j \rangle)^\top$ if $A_i = a$, and a row of zeros $\mathbf{0}^\top$ if $A_i \neq a$. Then the column-wise concatenation of the design matrices $\{\mathbf{D}_{j,a}\}_{a \in \{1, \dots, L\}}$, i.e., the $n \times d_j L$ matrix $\mathbf{D}_j = (\mathbf{D}_{j,1}; \mathbf{D}_{j,2}; \dots; \mathbf{D}_{j,L})$, defines the model matrix associated with the vectorized basis coefficient $\boldsymbol{\theta}_j \in \mathbb{R}^{d_j L}$, vectorized across $\{\boldsymbol{\theta}_{j,a}\}_{a \in \{1, \dots, L\}}$ in representation (12). We can then represent $g_j(\langle X_j, \widehat{\beta}_j \rangle, A)$ of (12), based on the sample data, by the length- n vector:

$$\mathbf{g}_j = \mathbf{D}_j \boldsymbol{\theta}_j \in \mathbb{R}^n \quad (14)$$

subject to the linear constraint (13) on the parameters $\boldsymbol{\theta}_j$. (Similarly, we can represent $h_k(Z_k, A)$ by a length- n vector.)

The linear constraint in (13) on $\boldsymbol{\theta}_j$ can be conveniently absorbed into the model matrix \mathbf{D}_j in (14) by reparametrization, which we describe next. We can find a $d_j L \times d_j(L-1)$ basis matrix $\mathbf{n}^{(j)}$ (that spans the null space of the linear constraint (13)), such that, if we set $\boldsymbol{\theta}_j = \mathbf{n}^{(j)} \widetilde{\boldsymbol{\theta}}_j$ for any arbitrary vector $\widetilde{\boldsymbol{\theta}}_j \in \mathbb{R}^{d_j(L-1)}$, then the vector $\boldsymbol{\theta}_j \in \mathbb{R}^{d_j L}$ automatically satisfies the constraint (13): $\boldsymbol{\pi}^{(j)} \boldsymbol{\theta}_j = \mathbf{0}$. Such a basis matrix $\mathbf{n}^{(j)}$ can be constructed by a QR decomposition of the matrix $\boldsymbol{\pi}^{(j)\top}$. Then representation (14) can be reparametrized, in terms of the unconstrained $\widetilde{\boldsymbol{\theta}}_j \in \mathbb{R}^{d_j(L-1)}$ by replacing \mathbf{D}_j in (14) with a reparametrized model matrix $\widetilde{\mathbf{D}}_j = \mathbf{D}_j \mathbf{n}^{(j)}$:

$$\mathbf{g}_j = \widetilde{\mathbf{D}}_j \widetilde{\boldsymbol{\theta}}_j. \quad (15)$$

Theorem 1, together with Section A.4 of Supporting Information, indicates that (for fixed $\beta_j = \widehat{\beta}_j$) the coordinate-wise minimizing function g_j of the right-hand side of (4) can be estimated based on the sample by:

$$\widehat{\mathbf{g}}_j = \left[1 - \frac{\lambda}{\sqrt{\frac{1}{n} \|\widehat{\mathbf{f}}_j\|^2}} \right]_+ \widehat{\mathbf{f}}_j \quad (16)$$

where

$$\widehat{\mathbf{f}}_j = \widetilde{\mathbf{D}}_j (\widetilde{\mathbf{D}}_j^\top \widetilde{\mathbf{D}}_j)^{-1} \widetilde{\mathbf{D}}_j^\top \widehat{\mathbf{R}}_j, \quad (17)$$

in which $\widehat{\mathbf{R}}_j = \mathbf{Y} - \sum_{j' \neq j} \widehat{\mathbf{g}}_{j'} - \sum_{k=1}^q \widehat{\mathbf{h}}_k$ corresponds to the estimated j th partial residual vector. (Similarly, we can represent the coordinate-wise minimizing function h_k in (8), based on the observed data by a length- n vector $\widehat{\mathbf{h}}_k$.) If we set each β_j equal to its corresponding estimate $\widehat{\beta}_j$ ($j = 1, \dots, p$), then based on the sample counterpart (16) of the coordinate-wise solution (5), a highly efficient coordinate descent algorithm can be conducted to optimize $\{g_j, j = 1, \dots, p\} \cup \{h_k, k = 1, \dots, q\}$ simultaneously. Let $\widehat{s}_j^{(\lambda)} := \left[1 - \lambda \sqrt{n} / \|\widehat{\mathbf{f}}_j\| \right]_+$ in (16) denote the soft-threshold shrinkage factor associated with the un-shrunk estimate $\widehat{\mathbf{f}}_j$ in (17). At convergence of the coordinate descent, we obtain a basis coefficient estimate of $\widetilde{\boldsymbol{\theta}}_j$ associated with representation (15):

$$\widehat{\widetilde{\boldsymbol{\theta}}}_j = \widehat{s}_j^{(\lambda)} (\widetilde{\mathbf{D}}_j^\top \widetilde{\mathbf{D}}_j)^{-1} \widetilde{\mathbf{D}}_j^\top \widehat{\mathbf{R}}_j, \quad (18)$$

which in turn implies an estimate of $\boldsymbol{\theta}_j$ in (14): $\widehat{\boldsymbol{\theta}}_j = (\widehat{\boldsymbol{\theta}}_{j,1}^\top, \widehat{\boldsymbol{\theta}}_{j,2}^\top, \dots, \widehat{\boldsymbol{\theta}}_{j,L}^\top)^\top = \mathbf{n}^{(j)} \widehat{\widetilde{\boldsymbol{\theta}}}_j$. Specifically, this gives an estimate of the treatment a -specific function $g_j(\cdot, a)$ ($a = 1, \dots, L$) in model (S.1):

$$\widehat{g}_j(\cdot, a) = \boldsymbol{\Psi}_j(\cdot)^\top \widehat{\boldsymbol{\theta}}_{j,a} \quad (a = 1, \dots, L) \quad (19)$$

estimated within the class of functions (12), for a given tuning parameter $\lambda \geq 0$ controlling the soft-threshold shrinkage factor $\widehat{s}_j^{(\lambda)}$ in (18), resulting in the functions $\{\widehat{g}_j, j = 1, \dots, p\} \cup \{\widehat{h}_k, k = 1, \dots, q\}$; this completes Step 1 of the alternating optimization procedure.

3.2.2 Step 2

We now consider a sample version of *Step 2* of the population algorithm that optimizes the coefficient functions $\{\beta_j, j = 1, \dots, p\}$ on the right-hand side of (4), for a fixed set of the component function estimates $\{\widehat{g}_j, j = 1, \dots, p\} \cup \{\widehat{h}_k, k = 1, \dots, q\}$ provided by *Step 1*. As an empirical approximation to (11), we consider

$$\underset{\beta_j \in \Theta}{\text{minimize}} \quad \sum_{i=1}^n \left\{ \widehat{R}_{ij} - \widehat{g}_j(\langle X_{ij}, \beta_j \rangle, A_i) \right\}^2 \quad (j = 1, \dots, p), \quad (20)$$

where \widehat{R}_{ij} is the i th element of $\widehat{\mathbf{R}}_j \in \mathbb{R}^n$ in (16). For this iterative estimation step, solving (20) can be approximately achieved based on a first-order Taylor series approximation of the term $\widehat{g}_j(\langle X_{ij}, \beta_j \rangle, A_i)$ at the current estimate, which we denote as $\widehat{\beta}_j^{(c)} \in \Theta$:

$$\begin{aligned} \sum_{i=1}^n \left\{ \widehat{R}_{ij} - \widehat{g}_j(\langle X_{ij}, \beta_j \rangle, A_i) \right\}^2 &\approx \sum_{i=1}^n \left\{ \widehat{R}_{ij} - \widehat{g}_j(\langle X_{ij}, \widehat{\beta}_j^{(c)} \rangle, A_i) - \dot{\widehat{g}}_j(\langle X_{ij}, \widehat{\beta}_j^{(c)} \rangle, A_i) \langle X_{ij}, \beta_j - \widehat{\beta}_j^{(c)} \rangle \right\}^2 \\ &= \sum_{i=1}^n \left\{ \widehat{R}_{ij}^* - \langle X_{ij}^*, \beta_j \rangle \right\}^2, \end{aligned} \quad (21)$$

where the “modified” residuals \widehat{R}_{ij}^* and the “modified” covariates X_{ij}^* are defined as:

$$\begin{aligned} \widehat{R}_{ij}^* &= \widehat{R}_{ij} - \widehat{g}_j(\langle X_{ij}, \widehat{\beta}_j^{(c)} \rangle, A_i) + \dot{\widehat{g}}_j(\langle X_{ij}, \widehat{\beta}_j^{(c)} \rangle, A_i) \langle X_{ij}, \widehat{\beta}_j^{(c)} \rangle & (i = 1, \dots, n), \\ X_{ij}^* &= \dot{\widehat{g}}_j(\langle X_{ij}, \widehat{\beta}_j^{(c)} \rangle, A_i) X_{ij} & (i = 1, \dots, n), \end{aligned} \quad (22)$$

in which each $\dot{\widehat{g}}_j(\cdot, a)$ denotes the first derivative of $\widehat{g}_j(\cdot, a)$ in (19) given by *Step 1*. We can perform a functional linear regression (e.g., Cardot et al., 2003) with scalar response \widehat{R}_{ij}^* and (functional) covariate X_{ij}^* to minimize the right-hand side of (21) over $\beta_j \in \Theta$. Specifically, the smooth coefficient function β_j in (21) is represented by a prespecified and normalized m_j -dimensional B -spline basis $B_j(s) = (b_{j1}(s), \dots, b_{jm_j}(s))^\top \in \mathbb{R}^{m_j}$, where m_j depends only on the sample size n (Fan et al., 2015):

$$\beta_j(s) = \sum_{r=1}^{m_j} b_{jr}(s) \gamma_{jr} \quad s \in [0, 1], \quad (23)$$

with an unknown basis coefficient vector $\gamma_j = (\gamma_{j1}, \gamma_{j2}, \dots, \gamma_{jm_j})^\top \in \mathbb{R}^{m_j}$. Suppose the function X_{ij} ($i = 1, \dots, n$) is discretized at points $\{s_l : 0 = s_1 < s_2 < \dots < s_{r_j} = 1\}$. Using the approximation $\langle X_{ij}, \widehat{\beta}_j^{(c)} \rangle \approx \sum_{l=1}^{r_j} \Delta_l X_{ij}(s_l) \widehat{\beta}_j^{(c)}(s_l)$ where Δ_l is the distance between two neighboring discretization points, we approximate \widehat{R}_{ij}^* and X_{ij}^* in (22). Let \mathbf{X}_j^* be the $n \times r_j$ matrix whose i th row is the discretized function $X_{ij}^*(s_l)$ ($l = 1, \dots, r_j$), and \mathbf{B}_j the $r_j \times m_j$ matrix whose l th row is the evaluated basis $B_j(s) \in \mathbb{R}^{m_j}$ at the l th point $s = s_l$ ($l = 1, \dots, r_j$). Given $\beta_j(s)$ discretized at the points $s = s_l$ ($l = 1, \dots, r_j$) in (23), we can represent the right-hand side of (21) as:

$$\|\mathbf{R}_j^* - \mathbf{U}_j^* \gamma_j\|^2, \quad (24)$$

where $\mathbf{R}_j^* := (R_{1j}^*, \dots, R_{nj}^*)^\top \in \mathbb{R}^n$ and $\mathbf{U}_j^* := \Delta \mathbf{X}_j^* \mathbf{B}_j$. Minimizing (24) over $\gamma_j \in \mathbb{R}^{m_j}$ for each j separately ($j = 1, \dots, p$) provides estimates $\{\widehat{\beta}_j, j = 1, \dots, p\}$ of the coefficient functions; here, the minimizer $\widehat{\gamma}_j$ for (24) is scaled to $\|\widehat{\gamma}_j\| = 1$, so that the resulting $\widehat{\beta}_j(s) = \sum_{r=1}^{m_j} b_{jr}(s) \widehat{\gamma}_{jr}$ ($s \in [0, 1]$) satisfies the identifiability constraint $\widehat{\beta}_j \in \Theta$. This completes *Step 2* of the alternating optimization procedure.

3.2.3 Initialization and convergence criterion

At the initial iteration, we need some estimates $\{\widehat{\beta}_j, j = 1, \dots, p\}$ of the single-index coefficient functions to initialize the single-indices $\{u_j = \langle \widehat{\beta}_j, \mathbf{X}_j \rangle, j = 1, \dots, p\}$, in order to perform *Step 1* (i.e., the coordinate-descent procedure) of the estimation procedure described in Section 3.2.1. At the initial iteration, we take $\widehat{\beta}_j(s) = 1$ ($s \in [0, 1]$), i.e., we take $u_j = \int_0^1 X_j(s) ds$ ($j = 1, \dots, p$), which corresponds to the common practice of taking a naïve scalar summary of each functional covariate. The proposed algorithm alternating between *Step 1* and *Step 2* terminates when the estimates $\{\widehat{\beta}_j, j = 1, \dots, p\}$ converge. To be specific, the algorithm terminates when $\max_{j=1, \dots, p, r=1, \dots, m_j} \|(\widehat{\gamma}_{jr} - \widehat{\gamma}_{jr}^{(c)})/\widehat{\gamma}_{jr}\|$ is less than a prespecified convergence tolerance; here, $\widehat{\gamma}_{jr}^{(c)}$ represents the current estimate for γ_{jr} in (23) at the beginning of *Step 1*, and $\widehat{\gamma}_{jr}$ is the estimate at the end of *Step 2*. We summarize the computational procedure in Algorithm 1.

Algorithm 1 Estimation of constrained functional additive models

- 1: **Input:** Data $\mathbf{Y} \in \mathbb{R}^n$, $\mathbf{A} \in \mathbb{R}^n$, $\mathbf{X}_j \in \mathbb{R}^n \times \mathbb{R}^{r_j}$ ($j = 1, \dots, p$), and $\lambda \geq 0$
 - 2: **Output:** Estimated functions $\{\widehat{\beta}_j, j = 1, \dots, p\}$ and $\{\widehat{g}_j, j = 1, \dots, p\}$
 - 3: Initialize $\widehat{\beta}_j(s) = 1$ ($s \in [0, 1]$) ($j = 1, \dots, p$).
 - 4: **while** until convergence of $\{\widehat{\beta}_j, j = 1, \dots, p\}$, **do** iterate between Step 1 and Step 2:
 - 5: (Step 1)
 - 6: Fix $\{\widehat{\beta}_j, j = 1, \dots, p\}$, and compute $\widetilde{\mathbf{D}}_j(\widetilde{\mathbf{D}}_j^\top \widetilde{\mathbf{D}}_j)^{-1} \widetilde{\mathbf{D}}_j^\top$ in (17) ($j = 1, \dots, p$).
 - 7: Initialize $\widehat{\mathbf{g}}_j = \mathbf{0} \in \mathbb{R}^n$ ($j = 1, \dots, p$).
 - 8: **while** until convergence of $\{\widehat{\mathbf{g}}_j, j = 1, \dots, p\}$, **do** iterate through $j = 1, \dots, p$:
 - 9: Compute the partial residual $\widehat{\mathbf{R}}_j = \mathbf{Y} - \sum_{j' \neq j} \widehat{\mathbf{g}}_{j'}$.
 - 10: Compute $\widehat{\mathbf{f}}_j$ in (17); then compute the thresholded estimate $\widehat{\mathbf{g}}_j$ in (16).
 - 11: (Step 2)
 - 12: Fix $\{\widehat{\mathbf{g}}_j, j = 1, \dots, p\}$ in (19), and solve (20) based on (24); update $\widehat{\beta}_j$ ($j = 1, \dots, p$).
-

In Algorithm 1, if the j th soft-threshold shrinkage factor $\widehat{s}_j^{(\lambda)} = \left[1 - \lambda\sqrt{n}/\|\widehat{\mathbf{f}}_j\|\right]_+$ in (16) is 0, then the associated X_j is absent from the model. Therefore, the corresponding coefficient function $\widehat{\beta}_j$ will not be updated, and this greatly reduces the computational cost when most of the shrinkage factors $\widehat{s}_j^{(\lambda)}$ are zeros. In Algorithm 1, the smoother matrix $\widetilde{\mathbf{D}}_j(\widetilde{\mathbf{D}}_j^\top \widetilde{\mathbf{D}}_j)^{-1} \widetilde{\mathbf{D}}_j^\top$ in (16) ($j = 1, \dots, p$) needs to be computed only once at the beginning of *Step 1* given fixed $\{\widehat{\beta}_j, j = 1, \dots, p\}$, and therefore the coordinate-descent updates in *Step 1* can be performed very efficiently (Fan et al., 2014). The sparsity tuning parameter $\lambda \geq 0$ can be chosen to minimize an estimate of the expected squared error of the estimated models over a dense grid of λ 's, estimated, for example, by a 10-fold cross-validation.

4 Simulation study

4.1 ITR estimation performance

In this section, we assess the optimal ITR estimation performance of the proposed method based on simulations. We generate n independent copies of p functional-valued covariates $\mathbf{X}_i = (X_{i1}, X_{i2}, \dots, X_{ip})$ ($i = 1, \dots, n$), where we use a 4-dimensional Fourier basis, $\boldsymbol{\Phi}(s) = (\sqrt{2} \sin(2\pi s), \sqrt{2} \cos(2\pi s), \sqrt{2} \sin(4\pi s), \sqrt{2} \cos(4\pi s))^\top \in \mathbb{R}^4$ ($s \in [0, 1]$), and random coefficients $\widetilde{\boldsymbol{\alpha}}_{ij} \in \mathbb{R}^4$, each independently following $\mathcal{N}(\mathbf{0}, \mathbf{I}_4)$, to form the functions $X_{ij}(s) = \boldsymbol{\Phi}(s)^\top \widetilde{\boldsymbol{\alpha}}_{ij}$ ($s \in [0, 1]$) ($i = 1, \dots, n; j = 1, \dots, p$). Then these covariates are evaluated at 50 equally spaced points $\{s_l\}_{l=1}^{50}$ between 0 and 1. We also generate n independent copies of q scalar covariates $\mathbf{Z}_i = (Z_{i1}, \dots, Z_{iq})^\top \in \mathbb{R}^q$ ($i = 1, \dots, n$), based on the multivariate normal distribution with each component having mean 0 and variance 1, with correlations between the components $\text{corr}(Z_{ij}, Z_{ik}) = 0.5^{|j-k|}$. We

generate the outcomes Y_i ($i = 1, \dots, n$) from:

$$Y_i = \epsilon_i + \delta \left\{ \sum_{j=1}^8 \sin(\langle \eta_j, X_{ij} \rangle) + \sum_{k=1}^8 \sin(Z_{ik}) \right\} + 4(A_i - 1.5) \left[\sin(\langle \beta_1, X_{i1} \rangle) - \sin(\langle \beta_2, X_{i2} \rangle) + \cos(Z_{i1}) - \cos(Z_{i2}) + \xi \{ \cos(\langle X_{i1}, X_{i2} \rangle) + \sin(Z_{i1} Z_{i2}) \} \right], \quad (25)$$

where the treatments $A_i \in \{1, 2\}$ are generated with equal probability, independently of $(\mathbf{X}_i, \mathbf{Z}_i)$ and $\epsilon_i \sim \mathcal{N}(0, 0.5^2)$. In (S.13), there are only four “signal” covariates (X_{i1}, X_{i2}, Z_{i1} and Z_{i2}) influencing the effect of A_i on Y_i (i.e., 4 treatment effect-modifiers). The other $p+q-4$ covariates are “noise” covariates not critical in optimizing ITRs. We set $p = q = 20$, therefore we consider a total of 40 pretreatment covariates in this example. In (S.13), we set the single-index coefficient functions, β_1 and β_2 , to be: $\beta_1(s) = \Phi(s)^\top (0.5, 0.5, 0.5, 0.5)$ and $\beta_2(s) = \Phi(s)^\top (0.5, -0.5, 0.5, -0.5)$, respectively (see Figure 2). We set the coefficient functions η_j ($j = 1, \dots, 8$) associated with the X_j “main” effect to be: $\eta_j(s) = \Phi(s)^\top \tilde{\eta}_j$, with each $\tilde{\eta}_j \in \mathbb{R}^4$ ($j = 1, \dots, 8$) following $\mathcal{N}(\mathbf{0}, \mathbf{I}_4)$ and then rescaled to a unit L^2 norm $\|\tilde{\eta}_j\| = 1$. The data model (S.13) is indexed by a pair (δ, ξ) . The parameter $\delta \in \{1, 2\}$ controls the contribution of the (\mathbf{X}, \mathbf{Z}) main effect component, $\delta \{ \sum_{j=1}^8 \sin(\langle \eta_j, X_{ij} \rangle) + \sum_{k=1}^8 \sin(Z_{ik}) \}$, to the variance of Y , in which $\delta = 1$ corresponds to a relatively *moderate* (\mathbf{X}, \mathbf{Z}) main effect (about 4 times greater than the interaction effect when $\xi = 0$) and $\delta = 2$ corresponds to a relatively *large* (\mathbf{X}, \mathbf{Z}) main effect (about 16 times greater than the interaction effect when $\xi = 0$). In (S.13), the parameter $\xi \in \{0, 1\}$ determines whether the A -by- (\mathbf{X}, \mathbf{Z}) interaction effect component has an additive regression structure ($\xi = 0$) of the form (S.1) or whether it deviates from an additive regression structure ($\xi = 1$). In the case of $\xi = 0$, the proposed CFAM (S.1) is correctly specified, whereas, for the case of $\xi = 1$, it is misspecified. For each simulation replication, we consider the following four approaches to estimating \mathcal{D}^{opt} :

1. The proposed approach (4), estimated via Algorithm 1, with the dimensions of the cubic B -spline basis for $\{g_j, h_k, \beta_j\}$ set at $d_j = d_k = m_j = 4 + (2n)^{1/5}$ (rounded to the closest integer), following Corollary 3 of Fan et al. (2015). The sparsity tuning parameter $\lambda > 0$ is chosen to minimize 10-fold cross-validated prediction error of the fitted models.
2. The functional linear regression approach of Ciarleglio et al. (2018),

$$\underset{\beta_j \in L^2[0,1], \alpha_k \in \mathbb{R}}{\text{minimize}} \quad E \left\{ Y - \sum_{j=1}^p \langle \beta_j, X_j \rangle (A - 1.5) - \sum_{k=1}^q \alpha_k Z_k (A - 1.5) \right\}^2 + \lambda \left\{ \sum_{j=1}^p (\|\beta_j\| + \rho_j \gamma_j^\top \mathbf{S}_j \gamma_j) + \sum_{k=1}^q |\alpha_k| \right\},$$

which tends to result in a sparse set $\{\beta_j\} \cup \{\alpha_k\}$, performing estimation based on representation (23) for the coefficient functions β_j given $m_j = 10$, with an associated $m_j \times m_j$ P -spline penalty matrix (\mathbf{S}_j) to ensure appropriate smoothness. The tuning parameters $\lambda > 0$ and $\rho = \rho_j > 0$ ($j = 1, \dots, p$) are chosen to minimize a 10-fold cross-validated prediction error (Ciarleglio et al., 2018), and the ITR is given by: $\widehat{\mathcal{D}}^{opt}(\mathbf{X}, \mathbf{Z}) = \arg \max_{a \in \{1, \dots, L\}} \{ \sum_{j=1}^p (a - 1.5) \langle \hat{\beta}_j, X_j \rangle + (a - 1.5) \sum_{k=1}^q \hat{\alpha}_k Z_k \}$. Since the component functions $\{g_j, h_k\}$ associated with Ciarleglio et al. (2018) are restricted to be linear (i.e., we restrict them to $g_j(\langle \beta_j, X_j \rangle, A) = \langle \beta_j, X_j \rangle (A - 1.5)$ and $h_k(Z_k, A) = \alpha_k Z_k (A - 1.5)$) corresponding to a special case of CFAM, we call the model of Ciarleglio et al. (2018), a CFAM with *linear* component functions (CFAM-lin) for the notational simplicity.

3. The outcome weighted learning (OWL; Zhao et al., 2012) method based on a linear kernel (OWL-lin), implemented in the R-package `DTRlearn`. Since there is no currently available OWL method that deals with functional covariates, we compute a scalar summary of each functional covariate, i.e., $\bar{X}_j = \int_0^1 X_j(s) ds \in \mathbb{R}$, and use \bar{X}_j along with the other scalar covariates Z_k as inputs to the augmented (residualized) OWL procedure. To improve its efficiency, we employ the augmented OWL approach of Liu et al. (2018), which amounts to pre-fitting a linear model for μ in (S.1) via Lasso (Tibshirani, 1996) and residualizing the response Y . The tuning parameter κ in Zhao et al. (2012) is chosen from the grid of (0.25, 0.5, 1, 2, 4) (the default setting of `DTRlearn`) based on a 10-fold cross-validation.

- The same approach as in 3 but based on a Gaussian radial basis function kernel (OWL-Gauss) in place of a linear kernel. The inverse bandwidth parameter σ_n^2 in Zhao et al. (2012) is chosen from the grid of $(0.01, 0.02, 0.04, \dots, 0.64, 1.28)$ and κ is chosen from the grid of $(0.25, 0.5, 1, 2, 4)$, based on a 10-fold cross-validation.

Throughout the paper, for CFAM and CFAM-lin, we fit the (\mathbf{X}, \mathbf{Z}) “main” effect on Y based on the (misspecified) linear model with the naïve scalar averages of X_j , i.e., \bar{X}_j , along with Z_k , fitted via Lasso with 10-fold cross-validation for the sparsity parameter and utilize the “residualized” response $Y - \hat{\mu}(\mathbf{X}, \mathbf{Z})$. For each simulation run, we estimate \mathcal{D}^{opt} from each of the above four methods based on a training set (of size $n \in \{250, 500\}$), and to evaluate these methods, we compute the value $V(\hat{\mathcal{D}}^{opt}) = E[E[Y|\mathbf{X}, \mathbf{Z}, A = \hat{\mathcal{D}}^{opt}(\mathbf{X}, \mathbf{Z})]]$ given each estimate $\hat{\mathcal{D}}^{opt}$, using a Monte Carlo approximation based on a separate random sample of size 10^3 . Since we know the true data generating model in simulation studies, the optimal \mathcal{D}^{opt} can be determined for each simulation run. Given each estimate $\hat{\mathcal{D}}^{opt}$ of \mathcal{D}^{opt} , we report $V(\hat{\mathcal{D}}^{opt}) - V(\mathcal{D}^{opt})$, as the performance measure of $\hat{\mathcal{D}}^{opt}$. A larger (i.e., less negative) value of the measure indicates better performance.

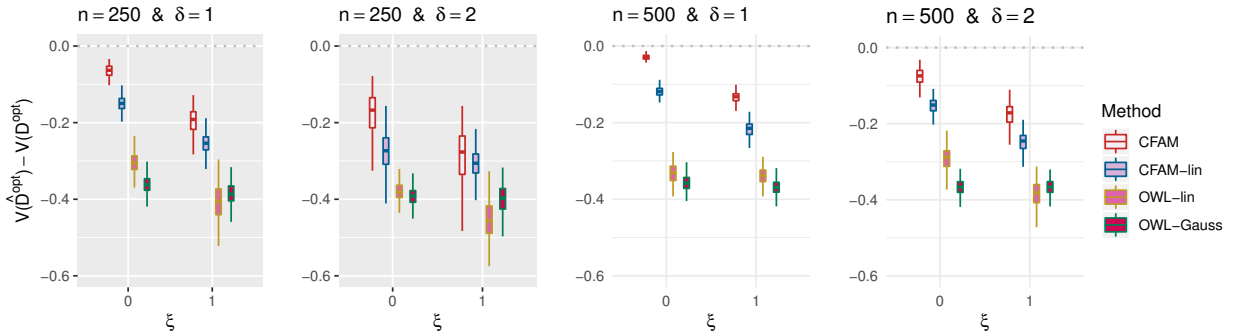


Figure 1: Boxplots obtained from 200 Monte Carlo simulations comparing 4 approaches to estimating \mathcal{D}^{opt} , given each scenario indexed by $\xi \in \{0, 1\}$, $\delta \in \{1, 2\}$ and $n \in \{250, 500\}$. The dotted horizontal line represents the optimal value corresponding to \mathcal{D}^{opt} .

In Figure S.1, we present boxplots, obtained from 200 simulation runs, of the normalized values $V(\hat{\mathcal{D}}^{opt})$ (normalized by the optimal values $V(\mathcal{D}^{opt})$) of the decision rules $\hat{\mathcal{D}}^{opt}$ estimated from the four approaches, for each combination of $n \in \{250, 500\}$, $\xi \in \{0, 1\}$ (corresponding to *correctly-specified* or *mis-specified* CFAM interaction models, respectively) and $\delta \in \{1, 2\}$ (corresponding to *moderate* or *large* main effects, respectively). The results in Figure S.1 indicate that the proposed method (CFAM) outperforms all other approaches. In particular, if the sample size is relatively large ($n = 500$), for a correctly-specified CFAM ($\xi = 0$) interaction underlying model, the proposed method gives a close-to-optimal performance in comparison to \mathcal{D}^{opt} . With nonlinearities present in the underlying model (S.13), CFAM-lin, which assumes a stringent linear structure on the interaction effect term, is outperformed by CFAM that utilizes the flexible component functions $g_j(\cdot, a)$ and $h_k(\cdot, a)$, while substantially outperforming the OWL-based approaches.

In Section A.5 of Supporting Information, we have also considered a similar set of experiments under a “linear” A -by- \mathbf{X} interaction effect, in which CFAM-lin outperforms CFAM, but by a relatively small amount, whereas if the underlying model deviates from the exact linear structure and $n = 500$, CFAM tends to outperform CFAM-lin. This suggests that, in the absence of prior knowledge about the form of the interaction effect, the more flexible CFAM that accommodates nonlinear treatment effect-modifications can be set as a default approach over CFAM-lin for optimizing ITRs. The estimated values of the OWL methods using linear and Gaussian kernels, respectively, are similar to each other, but both are outperformed by CFAM, even when CFAM is incorrectly specified (i.e., when $\xi = 1$), as the current OWL methods do not directly deal with the functional pretreatment covariates. When the (\mathbf{X}, \mathbf{Z}) “main” effect dominates the A -by- (\mathbf{X}, \mathbf{Z}) interaction effect (i.e., when $\delta = 2$), although the increased magnitude of this nuisance effect dampens the performance of all approaches to estimating \mathcal{D}^{opt} , the proposed approach outperforms all other methods.

Table 1: The root squared error (RSE) of the estimates $\widehat{\beta}_j$ for β_j ($j = 1, 2$) for varying sample size $n \in \{250, 500, 1000\}$, when the “main” effect of (\mathbf{X}, \mathbf{Z}) is moderate ($\delta = 1$) and large ($\delta = 2$), respectively.

	$\delta = 1$ (<i>Moderate</i> “main” effect)			$\delta = 2$ (<i>Large</i> “main” effect)		
n	250	500	1000	250	500	1000
RSE(β_1)	0.53(0.08)	0.34(0.02)	0.26(0.02)	0.60(0.14)	0.38(0.05)	0.29(0.03)
RSE(β_2)	0.53(0.06)	0.34(0.02)	0.27(0.01)	0.59(0.13)	0.39(0.07)	0.29(0.03)

In Table 1, we additionally illustrate the estimation performance for model parameters β_1 and β_2 when $\xi = 0$ (i.e., when CFAM is correctly specified) with varying $\delta \in \{1, 2\}$ and $n \in \{250, 500, 1000\}$, based on the root squared error $\text{RSE}(\beta_j) = \sqrt{\int (\widehat{\beta}_j(s) - \beta_j(s))^2 ds}$ ($j = 1, 2$). In Figure 2, we display typical CFAM estimates $\widehat{\beta}_j$ of β_j from 10 random samples, for each sample size n (for the case of $\delta = 1$). With sample size increasing, the estimators $\widehat{\beta}_j$ get close to the true coefficient functions β_j .

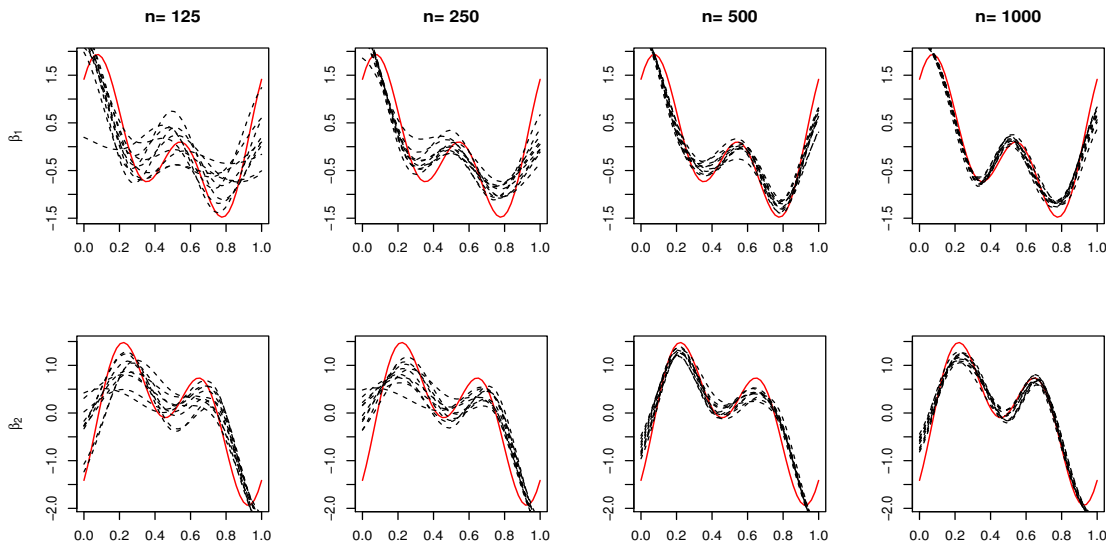


Figure 2: An illustration of typical 10 CFAM sample estimates $\widehat{\beta}_j(s)$ (black dashed curves) for the parameters $\beta_j(s)$ (the red solid curves), for $j = 1$ and 2 in the top and bottom panels, respectively, with a varying training sample size $n \in \{125, 250, 500, 1000\}$ for the case of $\delta = 1$.

4.2 Treatment effect-modifier variable selection performance

In this subsection, we will report simulation results for the treatment effect-modifier selection among $\{X_j, j = 1, \dots, p\} \cup \{Z_k, k = 1, \dots, q\}$. The complexity of the (\mathbf{X}, \mathbf{Z}) -by- A interaction terms of CFAM (S.1) can be summarized in terms of the size (cardinality) of the index set of $\{g_j, j = 1, \dots, p\} \cup \{h_k, k = 1, \dots, q\}$ that are not identically zero, each of which can be either correctly or incorrectly estimated to be equal to zero. As in Section 4.1, we generate 200 datasets based on (S.13), with varying $\xi \in \{0, 1\}$, $\delta \in \{1, 2\}$ and sample size $n \in \{50, 100, 200, \dots, 700, 800\}$ and $p = q = 20$, i.e., we consider a total of $p + q = 40$ potential treatment effect-modifiers, among which there are only 4 “true” treatment effect-modifiers.

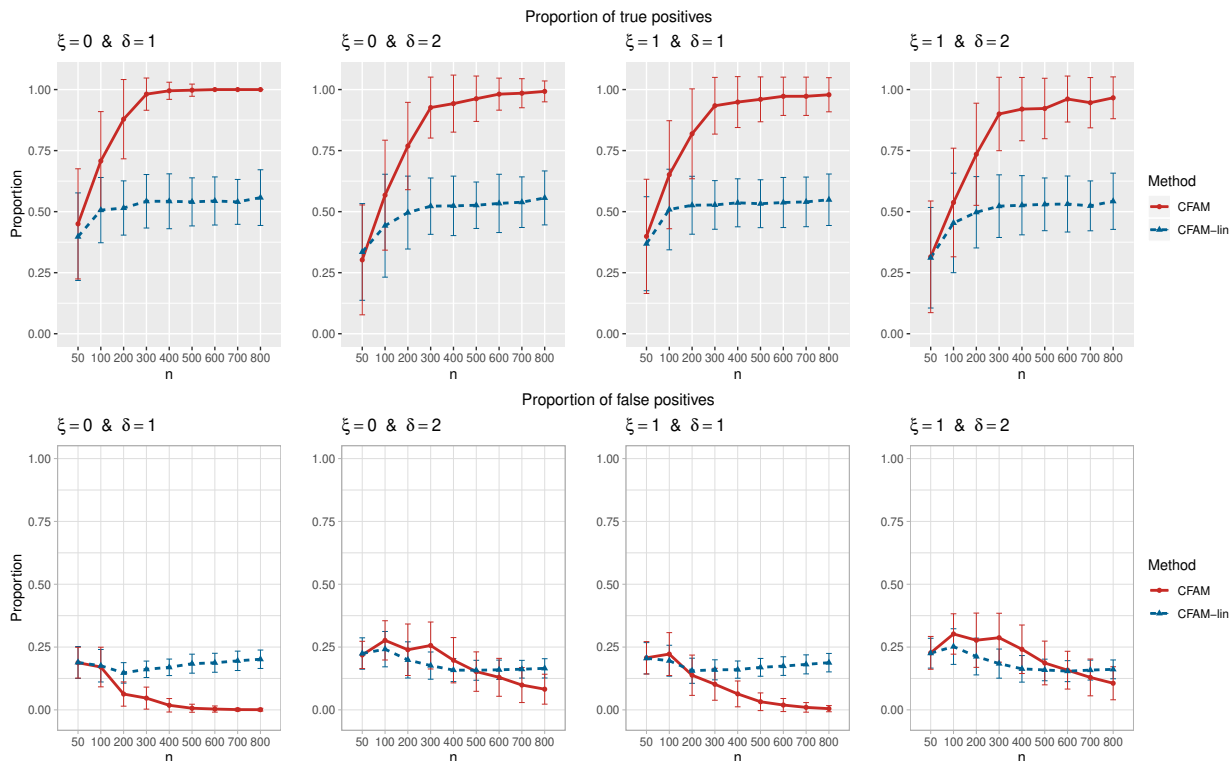


Figure 3: The proportion of the relevant covariates (i.e., the treatment effect-modifiers) correctly selected (the “true positives”; the top gray panels), and the “noise” covariates incorrectly selected (the “false positives”; the bottom white panels), respectively (and ± 1 standard deviation), with a varying sample size $n \in \{50, 100, 200, \dots, 800\}$, for each combination of $\xi \in \{0, 1\}$ and $\delta \in \{1, 2\}$.

Figure 3 summarizes the results of the treatment effect-modifier covariate selection performance with respect to the true/false positive rates (the top/bottom panels, respectively), comparing the proposed CFAM and the CFAM-lin of Ciarleglio et al. (2018). The results are reported as the averages (and ± 1 standard deviations) across the 200 simulated datasets, for each simulation scenario. Figure 3 illustrates that the proportion of *correct* selection out of the 4 *true* treatment effect-modifiers (i.e., the “true positive” rate; the top gray panels) of CFAM (the red solid curves) tends to 1, as n increases from $n = 50$ to $n = 800$, whereas the proportion of *incorrect* selection (i.e., the “false positive” rate; the bottom white panels) out of the 36 *irrelevant* “noise” covariates tends to 0; these proportions tend to either 1 or 0 quickly for *moderate* main effect ($\delta = 1$) scenarios compared to *large* main effect ($\delta = 2$) scenarios. On the other hand, the proportion of correct selections for CFAM-lin (the blue dotted curves), even with a large n , tends to be only around 0.55, due to the stringent linear model assumption on the form of the (\mathbf{X}, \mathbf{Z}) -by- A interaction effect.

5 Application

In this section, we illustrate the utility of CFAM for optimizing ITRs, using data from an RCT (Trivedi et al., 2016) comparing an antidepressant and placebo for treating major depressive disorder. The study collected various scalar and functional patient characteristics at baseline, including electroencephalogram (EEG) data. Study participants were randomized to either placebo ($A = 1$) or an antidepressant (sertraline) ($A = 2$). Subjects were monitored for 8 weeks after initiation of treatment. The primary endpoint of interest was the Hamilton Rating Scale for Depression (HRSD) score at week 8. The outcome Y was taken to be the improvement in symptoms severity from baseline to week 8 taken as the difference: week 0 HRSD score - week 8 HRSD score (larger values of the outcome Y are considered desirable).

There were $n = 180$ subjects. We considered $p = 19$ pretreatment functional covariates consisting of the current source density (CSD) amplitude spectrum curves over the Alpha frequency range (observed while the participants’ eyes were open), measured from a subset of EEG channels from a total of 72 EEG electrodes which gives a fairly good spatial coverage of the scalp. The locations for these 19 electrodes are indicated in the top panel of Figure 4. The Alpha frequency band (8 to 12 Hz) considered as a potential biomarker of antidepressant response (e.g., Wade and Iosifescu, 2016) was scaled to $[0, 1]$, hence each of the functional covariates $X = (X_1(s), \dots, X_{19}(s))$ was defined on the interval $[0, 1]$. We also considered $q = 5$ baseline scalar covariates consisting of the week 0 HRSD score (Z_1), sex (Z_2), age at evaluation (Z_3), word fluency (Z_4) and Flanker accuracy (Z_5) cognitive test scores, which were identified as predictors of differential treatment response in a previous study (Park et al., 2020c). In this dataset, 49% of the subjects were randomized to the sertraline ($A = 2$). The average outcomes Y for the sertraline and placebo groups were 7.41 and 6.29, respectively. The means (and standard deviations) of Z_1 , Z_3 , Z_4 and Z_5 were 18.59 (4.44), 37.7 (13.57), 38 (11.42) and 0.19 (0.11), respectively, and 67% of the subjects were female.

The proposed CFAM approach (4) selected two functional covariates: “C3” (X_4) and “P3” (X_5) (the selected electrodes are indicated by the red dashed circles in the top panel of Figure 4), and a scalar covariate: “Flanker accuracy test” (Z_5). In the first column of Figure 4, we display CSD curves corresponding to the selected two functional covariates, $X_4(s)$ and $X_5(s)$, from the 180 subjects. In the second column of Figure 4, we display the estimated coefficient functions, $\hat{\beta}_4(s)$ and $\hat{\beta}_5(s)$ (with 95% confidence bands conditional on the j th partial residual and the j th component function \hat{g}_j), associated with those selected covariates.

The coefficient functions $\hat{\beta}_j(s)$ summarizing the $X_j(s)$ lead to data-driven indices $u_j = \langle \hat{\beta}_j, X_j \rangle \in \mathbb{R}$ that are linked to differential treatment response by two estimated nonzero component functions, $\hat{g}_j(u_j, A)$ ($j = 4, 5$) in this example. In Figure 4, the fitted component functions, $\hat{g}_j(u_j, A)$ associated with the placebo $A = 1$ (in the third column) and the active drug $A = 2$ (in the fourth column), are displayed, along with the corresponding partial residuals. Roughly put, in Figure 4, the placebo ($A = 1$) effect tends to increase with the index u_j ($j = 4, 5$) whereas the sertraline ($A = 2$) effect decreases with the index. In the second column of Figure 4, both β_4 and β_5 put a bulk of their negative weight on lower frequencies (8 to 9 Hz), meaning that patients whose CSD values are small in those frequency regions would have large values of $\langle \beta_j, X_j \rangle$, over the values which the placebo effects are predicted to be relatively strong, in comparison to the sertraline effects.

To evaluate the performance of ITRs ($\hat{\mathcal{D}}^{opt}$) estimated from the four different approaches described in Section 4, we randomly split the data into a training set and a testing set (of size \tilde{n}) using a ratio of 5 : 1, replicated 500 times, each time estimating an ITR $\hat{\mathcal{D}}^{opt}$ based on the training set, and its “value” $V(\hat{\mathcal{D}}^{opt}) = E[E[Y|\mathbf{X}, \mathbf{Z}, A = \hat{\mathcal{D}}^{opt}(\mathbf{X}, \mathbf{Z})]]$, by an inverse probability weighted estimator (Murphy, 2005) $\hat{V}(\hat{\mathcal{D}}^{opt}) = \sum_{i=1}^n Y_i I_{(A_i = \hat{\mathcal{D}}^{opt}(\mathbf{X}_i, \mathbf{Z}_i))} / \sum_{i=1}^n I_{(A_i = \hat{\mathcal{D}}^{opt}(\mathbf{X}_i, \mathbf{Z}_i))}$, computed based on the testing set (of size \tilde{n}). For comparison, we also include two naïve rules: treating all patients with placebo (“All PBO”) and treating all patients with the active drug (“All DRUG”), each regardless of the individual patient’s characteristics (\mathbf{X}, \mathbf{Z}). The resulting boxplots obtained from the 500 random splits are illustrated in Figure 6.

The results in Figure 6 demonstrate that CFAM and CFAM-lin perform at a similar level, showing a clear advantage over the both OWL-lin and OWL-Gauss, suggesting that regression utilizing the functional nature of the EEG measurements, that targets the treatment-by-functional covariates interactions is well-suited in this example. Specifically, in Figure 6, the superiority of CFAM (or CFAM-lin) over the policy of treating everyone with the drug (All DRUG) was of similar magnitude of the superiority of All DRUG over All PBOs. This suggests that accounting for patient characteristics can help treatment decisions. In this example, as can be observed from the third and fourth columns of Figures 4 and 5, the estimated nonlinear treatment effect-modification is rather modest. As a result, the performances of CFAM and CFAM-lin are comparable to each other. However, as demonstrated in Section 4, the more flexible CFAM can be employed as a default approach over CFAM-lin, allowing for potentially essential nonlinearities in treatment effect-modification.

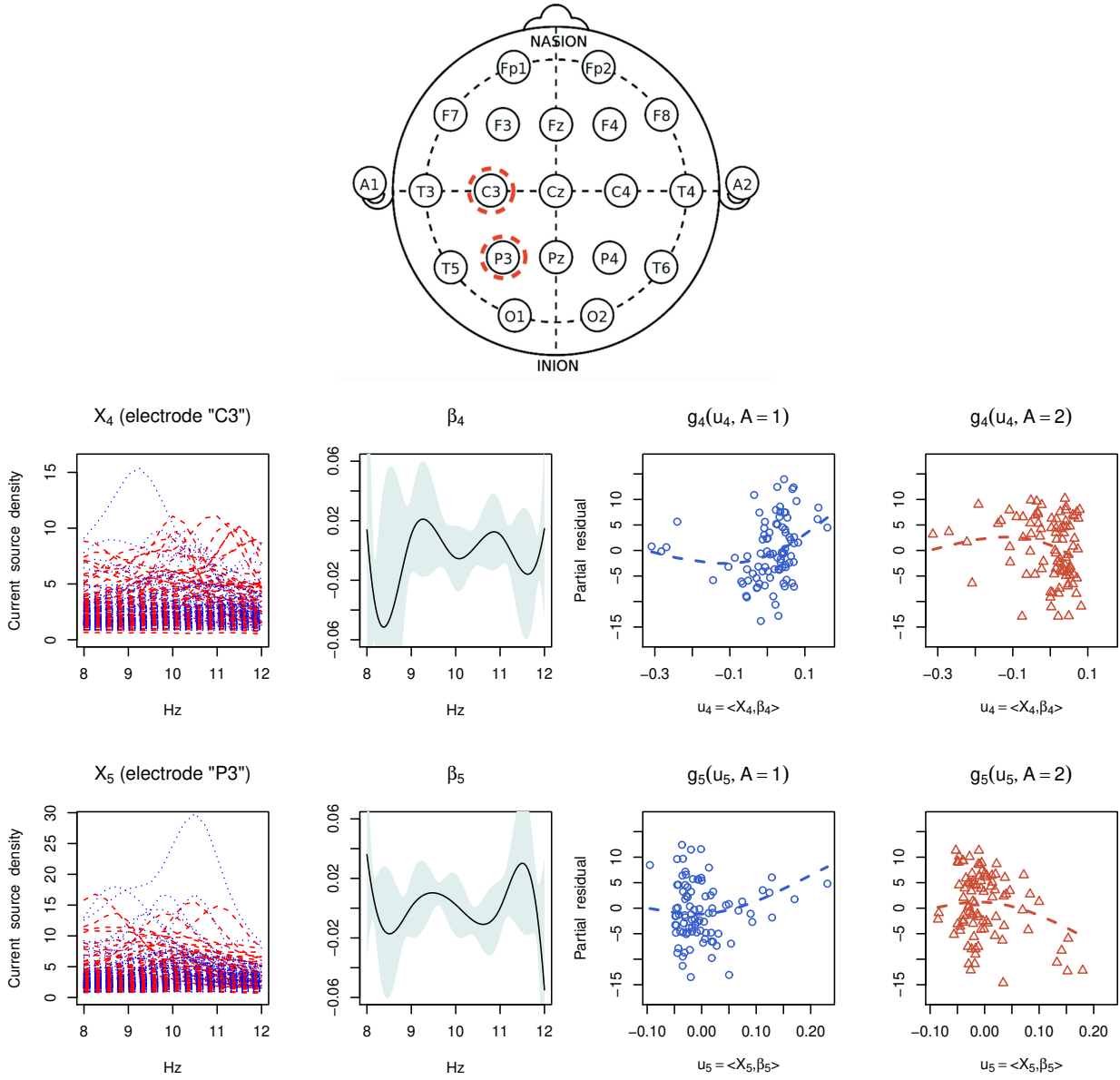


Figure 4: **Top:** The locations for the 19 electrode channels (“A1” and “A2” were not used). Those marked in red circles are the selected electrodes from the proposed approach: “C3” and “P3”. **Bottom:** First column: observed current source density (CSD) curves from the selected channels X_4 (“C3”) and X_5 (“P3”), over the Alpha band (8 to 12 Hz). Second column: the estimated single-index coefficient functions (β_4 and β_5) for the selected channels X_4 and X_5 (and the associated 95% confidence bands, conditioning on the j th partial residual and the j th component function \hat{g}_j). Third and fourth columns: the scatter plots of the (j th; $j = 4, 5$, top and bottom, respectively) partial residuals vs. the estimated single-indices $u_4 = \langle X_4, \beta_4 \rangle$ and $u_5 = \langle X_5, \beta_5 \rangle$, respectively, for the placebo $A = 1$ (third column, blue circles) and sertraline $A = 2$ (fourth column, red triangles) treated individuals, with the estimated treatment-specific component functions $g_j(u_j, A)$ ($A = 1, 2$) ($j = 4, 5$) (the dashed curves) overlaid.

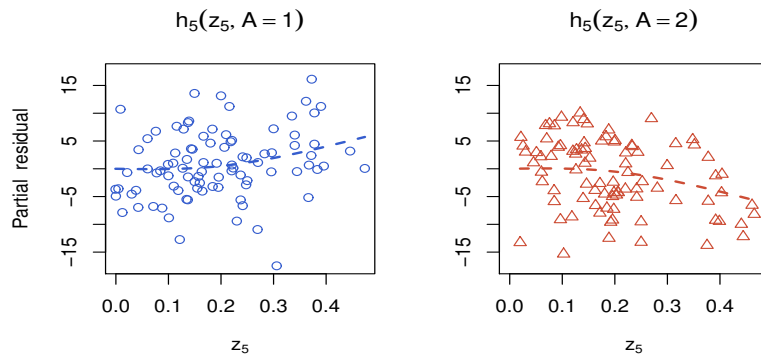


Figure 5: The scatter plots of the k th partial residual vs. the k th scalar covariate, for the selected 5th scalar covariate Z_5 “Flanker accuracy test score,” for the placebo $A = 1$ (first column, blue circles) and sertraline $A = 2$ (second column, red triangles) treated individuals, with the estimated treatment-specific component functions $h_5(z_5, A)$ ($A = 1, 2$) (the dashed curves) overlaid.

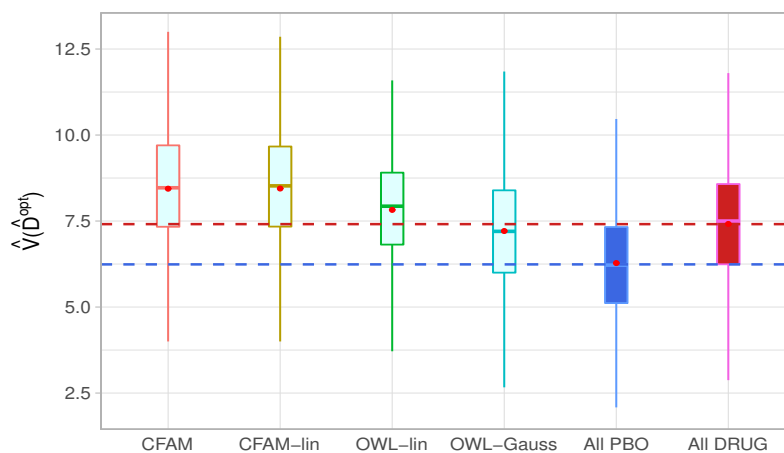


Figure 6: Boxplots of the estimated values of the treatment rules \hat{D}^{opt} estimated from 6 approaches, obtained from 500 randomly split testing sets. Higher values are preferred.

6 Discussion

We have developed a functional additive regression approach specifically focused on extracting possibly nonlinear pertinent interaction effects between treatment and multiple functional/scalar covariates, which is of paramount importance in developing effective ITRs for precision medicine. This is accomplished by imposing appropriate structural constraints, performing treatment effect-modifier selection and extracting one-dimensional functional indices. The estimation approach utilizes an efficient coordinate-descent for the component functions and a functional linear model estimation procedure for the coefficient functions. The proposed functional regression for ITRs extends existing methods by incorporating possibly nonlinear treatment-by-functional covariates interactions. Encouraged by our simulation results and the application, future work will investigate the asymptotic properties of the method related to variable selection and estimation consistency, and a hypothesis testing framework for significant interactions between treatment and functional covariates.

SUPPLEMENTARY MATERIAL

Supplementary Material at the end of the document provides additional technical details referred to in the main paper, including the proof of Theorem 1. Supplementary Material also presents additional simulation examples, including a set of simulation experiments with a “linear” A -by- (\mathbf{X}, \mathbf{Z}) interaction effect scenario.

R-package: R-package `famTEMsel` (Functional Additive Models for Treatment Effect-Modifier Selection) contains R-codes to perform the methods proposed in the article, and is publicly available on [GitHub](#) ([syhyunpark/famTEMsel](#)).

Acknowledgments

This work was supported by National Institute of Health (NIH) grant 5 R01 MH099003.

Conflict of interest

None declared.

References

- Cardot, H., Ferraty, F., and Sarda, P. (2003). Spline estimators for the functional linear model. *Statistica Sinica* **13**, 571–592.
- Ciarleglio, A., Petkova, E., Ogden, R. T., and Tarpey, T. (2015). Treatment decisions based on scalar and functional baseline covariates. *Biometrics* **71**, 884–894.
- Ciarleglio, A., Petkova, E., Ogden, R. T., and Tarpey, T. (2018). Constructing treatment decision rules based on scalar and functional predictors when moderators of treatment effect are unknown. *Journal of Royal Statistical Society: Series C* **67**, 1331–1356.
- Ciarleglio, A., Petkova, E., Tarpey, T., and Ogden, R. T. (2016). Flexible functional regression methods for estimating individualized treatment rules. *Stat* **5**, 185–199.
- Fan, Y., Foutz, N., James, G. M., and Jank, W. (2014). Functional response additive model estimation with online virtual stock markets. *The Annals of Applied Statistics* **8**, 2435–2460.

- Fan, Y., James, G. M., and Radchanko, P. (2015). Functional additive regression. *The Annals of Statistics* **43**, 2296–2325.
- Hastie, T. and Tibshirani, R. (1999). *Generalized Additive Models*. Chapman & Hall Ltd.
- Jeng, X., Lu, W., and Peng, H. (2018). High-dimensional inference for personalized treatment decision. *Electronic Journal of Statistics* **12**, 2074–2089.
- Kang, C., Janes, H., and Huang, Y. (2014). Combining biomarkers to optimize patient treatment recommendations. *Biometrics* **70**, 696–707.
- Laber, E. B. and Zhao, Y. (2015). Tree-based methods for individualized treatment regimes. *Biometrika* **102**, 501–514.
- Liu, Y., Wang, Y., Kosorok, M. R., Zhao, Y., and Zeng, D. (2018). Augmented outcome-weighted learning for estimating optimal dynamic treatment regimens. *Statistics in Medicine* **37**, 3776–3788.
- Lu, W., Zhang, H., and Zeng, D. (2011). Variable selection for optimal treatment decision. *Statistical Methods in Medical Research* **22**, 493–504.
- McKeague, I. and Qian, M. (2014). Estimation of treatment policies based on functional predictors. *Statistica Sinica* **24**, 1461–1485.
- McLean, M., Hooker, G., Staicu, A., Scheipel, F., and Ruppert, D. (2014). Functional generalized additive models. *Journal of Computational and Graphical Statistics* **23**, 249–269.
- Morris, J. S. (2015). Functional regression. *Annual Review of Statistics and Its Application* **2**, 321–359.
- Murphy, S. A. (2005). A generalization error for q-learning. *Journal of Machine Learning* **6**, 1073–1097.
- Park, H., Petkova, E., Tarpey, T., and Ogden, R. T. (2020a). A constrained single-index regression for estimating interactions between a treatment and covariates. *Biometrics*. <https://doi.org/10.1111/biom.13320>.
- Park, H., Petkova, E., Tarpey, T., and Ogden, R. T. (2020b). A single-index model with multiple-links. *Journal of Statistical Planning and Inference* **205**, 115–128.
- Park, H., Petkova, E., Tarpey, T., and Ogden, R. T. (2020c). A sparse additive model for treatment effect-modifier selection. *Biostatistics*. *kxaa032*, <https://doi.org/10.1093/biostatistics/kxaa032>.
- Petkova, E., Park, H., Ciarleglio, A., Ogden, R., and Tarpey, T. (2020). Optimising treatment decision rules through generated effect modifiers: a precision medicine tutorial. *BJPsych Open* **6**, 1–7.
- Qian, M. and Murphy, S. A. (2011). Performance guarantees for individualized treatment rules. *The Annals of Statistics* **39**, 1180–1210.
- Ramsay, J. O. and Silverman, B. W. (1997). *Functional Data Analysis*. Springer, New York.
- Ravikumar, P., Lafferty, J., Liu, H., and Wasserman, L. (2009). Sparse additive models. *Journal of Royal Statistical Society: Series B* **71**, 1009–1030.
- Shi, C., Song, R., and Lu, W. (2016). Robust learning for optimal treatment decision with np-dimensionality. *Electronic Journal of Statistics* **10**, 2894–2921.
- Song, R., Kosorok, M., Zeng, D., Zhao, Y., Laber, E. B., and Yuan, M. (2015). On sparse representation for optimal individualized treatment selection with penalized outcome weighted learning. *Stat* **4**, 59–68.
- Tian, L., Alizadeh, A., Gentles, A., and Tibshirani, R. (2014). A simple method for estimating interactions between a treatment and a large number of covariates. *Journal of the American Statistical Association* **109**, 1517–1532.

- Tibshirani, R. (1996). Regression shrinkage and selection via the lasso. *Journal of the Royal Statistical Society: Series B (Statistical Methodology)* **58**, 267–288.
- Trivedi, M., McGrath, P., Fava, M., Parsey, R., Kurian, B., Phillips, M., Oquendo, M., Bruder, G., Pizzagalli, D., Toups, M., Cooper, C., Adams, P., Weyandt, S., Morris, D., Grannemann, B., Ogden, R., Buckner, R., McInnis, M., Kraemer, H., Petkova, E., Carmody, T., and Weissman, M. (2016). Establishing moderators and biosignatures of antidepressant response in clinical care (EMBARC): Rationale and design. *Journal of Psychiatric Research* **78**, 11–23.
- Wade, E. and Iosifescu, D. (2016). Using electroencephalography for treatment guidance in major depressive disorder. *Biological Psychiatry: Cognitive Neuroscience and Neuroimaging* **1**, 411–422.
- Zhang, B., Tsiatis, A. A., Davidian, M., Zhang, M., and Laber, E. (2012). Estimating optimal treatment regimes from classification perspective. *Stat* **1**, 103–114.
- Zhao, Y., Laber, E., Ning, Y., Saha, S., and Sands, B. (2019). Efficient augmentation and relaxation learning for individualized treatment rules using observational data. *Journal of Machine Learning Research* **20**, 1–23.
- Zhao, Y., Zeng, D., Rush, A. J., and Kosorok, M. R. (2012). Estimating individualized treatment rules using outcome weighted learning. *Journal of the American Statistical Association* **107**, 1106–1118.
- Zhao, Y., Zheng, D., Laber, E. B., and Kosorok, M. R. (2015). New statistical learning methods for estimating optimal dynamic treatment regimes. *Journal of the American Statistical Association* **110**, 583–598.

SUPPLEMENTARY MATERIAL

Appendix A: Technical details and additional simulations

A.1. Description of the constrained least squares criterion in Section 2.1

In Section 2 of the main manuscript, we introduce the constrained functional additive model (CFAM) for the (\mathbf{X}, \mathbf{Z}) -by- A interaction effect:

$$Y = \mu(\mathbf{X}, \mathbf{Z}) + \sum_{j=1}^p g_j(\langle X_j, \beta_j \rangle, A) + \sum_{k=1}^q h_k(Z_k, A) + \epsilon, \quad (\text{S.1})$$

with $\beta_j \in \Theta$, subject to the constraint on the component functions $g_j \in \mathcal{H}_j^{(\beta_j)}$ ($j = 1, \dots, p$) and $h_k \in \mathcal{H}_k$ ($k = 1, \dots, q$):

$$\begin{aligned} E[g_j(\langle X_j, \beta_j \rangle, A)|X_j] &= 0 \quad (\text{almost surely}) \quad (\forall \beta_j \in \Theta) \quad (j = 1, \dots, p) \quad \text{and} \\ E[h_k(Z_k, A)|Z_k] &= 0 \quad (\text{almost surely}) \quad (k = 1, \dots, q), \end{aligned} \quad (\text{S.2})$$

in which the expectation is taken with respect to the distribution of A given X_j (or Z_k), and $\epsilon \in \mathbb{R}$ is a mean zero noise with finite variance, and the form of the squared integrable functional μ in (S.1) is left unspecified.

Under model (S.1) subject to (S.2), the “true” (i.e., optimal) functional components, which we denote by $\{g_j^*, j = 1, \dots, p\} \cup \{\beta_j^*, j = 1, \dots, p\} \cup \{h_k^*, k = 1, \dots, q\}$ that constitute the (\mathbf{X}, \mathbf{Z}) -by- A interaction effect, can be specified and viewed as the solution to the following constrained least squares problem:

$$\begin{aligned} \{g_j^*, \beta_j^*, h_k^*\} &= \underset{g_j \in \mathcal{H}_j^{(\beta_j)}, \beta_j \in \Theta, h_k \in \mathcal{H}_k}{\operatorname{argmin}} \quad E \left[\left\{ Y - \mu(\mathbf{X}, \mathbf{Z}) - \sum_{j=1}^p g_{j,A}(\langle X_j, \beta_j \rangle) - \sum_{k=1}^q h_{k,A}(Z_k) \right\}^2 \right] \\ &\text{subject to} \quad E[g_{j,A}(\langle X_j, \beta_j \rangle)|X_j] = 0 \quad \forall \beta_j \in \Theta \quad (j = 1, \dots, p) \quad \text{and} \\ &\quad E[h_{k,A}(Z_k)|Z_k] = 0 \quad (k = 1, \dots, q), \end{aligned} \quad (\text{S.3})$$

in which $\mu(\mathbf{X}, \mathbf{Z})$ is the “main” effect component appeared in model (S.1) (and is considered as fixed in (S.3)). In particular, on the right-hand side of (S.3), the expected squared error criterion term can be expanded as:

$$\begin{aligned} &\underset{g_j \in \mathcal{H}_j^{(\beta_j)}, \beta_j \in \Theta, h_k \in \mathcal{H}_k}{\operatorname{argmin}} \quad \mathbb{E} \left[\left\{ Y - \sum_{j=1}^p g_{j,A}(\langle X_j, \beta_j \rangle) - \sum_{k=1}^q h_{k,A}(Z_k) \right\}^2 + 2\mu(\mathbf{X}, \mathbf{Z}) \left\{ \sum_{j=1}^p g_{j,A}(\langle X_j, \beta_j \rangle) + \sum_{k=1}^q h_{k,A}(Z_k) \right\} \right] \\ &= \underset{g_j \in \mathcal{H}_j^{(\beta_j)}, \beta_j \in \Theta, h_k \in \mathcal{H}_k}{\operatorname{argmin}} \quad \mathbb{E} \left[\left\{ Y - \sum_{j=1}^p g_{j,A}(\langle X_j, \beta_j \rangle) - \sum_{k=1}^q h_{k,A}(Z_k) \right\}^2 + 2\mu(\mathbf{X}, \mathbf{Z}) \mathbb{E} \left[\sum_{j=1}^p g_{j,A}(\langle X_j, \beta_j \rangle) + \sum_{k=1}^q h_{k,A}(Z_k) | \mathbf{X}, \mathbf{Z} \right] \right] \\ &= \underset{g_j \in \mathcal{H}_j^{(\beta_j)}, \beta_j \in \Theta, h_k \in \mathcal{H}_k}{\operatorname{argmin}} \quad \mathbb{E} \left[\left\{ Y - \sum_{j=1}^p g_{j,A}(\langle X_j, \beta_j \rangle) - \sum_{k=1}^q h_{k,A}(Z_k) \right\}^2 \right], \end{aligned}$$

in which the second line follows from an application of the iterated expectation rule to condition on (\mathbf{X}, \mathbf{Z}) on the second term on the first line, and the third line follows from the constraint imposed in (S.3), that is, $\mathbb{E}[g_{j,A}(\langle X_j, \beta_j \rangle)|X_j] = 0$, $\forall \beta_j \in \Theta$ ($j = 1, \dots, p$) and $\mathbb{E}[h_{k,A}(Z_k)|Z_k] = 0$ ($k = 1, \dots, q$), which makes the second term on the second line of the above expression vanish to zero.

Since the minimization in (S.3) is in terms of $\{g_j, \beta_j, h_k\}$, the right-hand side of (S.3) can then be reduced to:

$$\begin{aligned} \{g_j^*, \beta_j^*, h_k^*\} &= \underset{g_j \in \mathcal{H}_j^{(\beta_j)}, \beta_j \in \Theta, h_k \in \mathcal{H}_k}{\operatorname{argmin}} \quad E \left[\left\{ Y - \sum_{j=1}^p g_j(\langle X_j, \beta_j \rangle, A) - \sum_{k=1}^q h_k(Z_k, A) \right\}^2 \right] \\ &\text{subject to} \quad E[g_j(\langle X_j, \beta_j \rangle, A)|X_j] = 0 \quad \forall \beta_j \in \Theta \quad (j = 1, \dots, p) \quad \text{and} \\ &\quad E[h_k(Z_k, A)|Z_k] = 0 \quad (k = 1, \dots, q), \end{aligned} \quad (\text{S.4})$$

which is as appeared in the representation (3) of the main manuscript.

A.2. Proof of Theorem 1

In this subsection, we provide the proof of Theorem 1 in Section 3.1 of the main manuscript. In order to simplify the exposition, we focus on the derivation of the minimizing functions $g_j \in \mathcal{H}_j^{(\beta_j)}$ ($j = 1, \dots, p$) associated with the functional covariates X_j ($j = 1, \dots, p$), only. The minimizing functions $h_k \in \mathcal{H}_k$ ($k = 1, \dots, q$) associated with the scalar covariates Z_k ($k = 1, \dots, q$) are derived in the similar way. Further, for fixed $\beta_j \in \Theta$ ($j = 1, \dots, p$), we write $X_{\beta_j} = \langle X_j, \beta_j \rangle \in \mathbb{R}$ ($j = 1, \dots, p$), for notational simplicity.

The squared error criterion on the right-hand side of (S.4) is

$$\begin{aligned}
\mathbb{E} \left[\left\{ Y - \sum_{j=1}^p g_j(X_{\beta_j}, A) \right\}^2 \right] &\propto \mathbb{E} \left[Y \sum_{j=1}^p g_j(X_{\beta_j}, A) - \left\{ \sum_{j=1}^p g_j(X_{\beta_j}, A) \right\}^2 / 2 \right] \quad (\text{with respect to } \{g_j\}) \\
&= \mathbb{E} \left[\left\{ \mu(\mathbf{X}) + \sum_{j=1}^p g_j^*(X_{\beta_j^*}, A) \right\} \sum_{j=1}^p g_j(X_{\beta_j}, A) - \left\{ \sum_{j=1}^p g_j(X_{\beta_j}, A) \right\}^2 / 2 \right] \\
&= \mathbb{E} \left[\mu(\mathbf{X}) \sum_{j=1}^p g_j(X_{\beta_j}, A) \right] + \mathbb{E} \left[\left\{ \sum_{j=1}^p g_j^*(X_{\beta_j^*}, A) \right\} \left\{ \sum_{j=1}^p g_j(X_{\beta_j}, A) \right\} - \left\{ \sum_{j=1}^p g_j(X_{\beta_j}, A) \right\}^2 / 2 \right] \\
&= \mathbb{E} \left[\left\{ \sum_{j=1}^p g_j^*(X_{\beta_j^*}, A) \right\} \left\{ \sum_{j=1}^p g_j(X_{\beta_j}, A) \right\} - \left\{ \sum_{j=1}^p g_j(X_{\beta_j}, A) \right\}^2 / 2 \right], \tag{S.5}
\end{aligned}$$

where the last equality follows from the constraint $\mathbb{E}[g_j(X_{\beta_j}, A) | X_j] = 0$ ($j = 1, \dots, p$) in (S.4) imposed on $\{g_j\}$, which implies $\mathbb{E}[\mu(\mathbf{X}) \{ \sum_{j=1}^p g_j(X_{\beta_j}, A) \}] = \mathbb{E}[\mathbb{E}[\mu(\mathbf{X}) \{ \sum_{j=1}^p g_j(X_{\beta_j}, A) \} | \mathbf{X}]] = \mathbb{E}[\mu(\mathbf{X}) \sum_{j=1}^p \mathbb{E}[g_j(X_{\beta_j}, A) | X_j]] = 0$. From (S.5), for fixed $\{\beta_j, j = 1, \dots, p\}$, we can rewrite the squared error criterion in (S.4) by (omitting the components associated with the scalar covariates):

$$\operatorname{argmin}_{\{g_j \in \mathcal{H}_j^{(\beta_j)}\}} \mathbb{E} \left[\left(Y - \sum_{j=1}^p g_j(X_{\beta_j}, A) \right)^2 \right] = \operatorname{argmin}_{\{g_j \in \mathcal{H}_j^{(\beta_j)}\}} \mathbb{E} \left[\left(\sum_{j=1}^p g_j^*(X_{\beta_j^*}, A) - \sum_{j=1}^p g_j(X_{\beta_j}, A) \right)^2 \right]. \tag{S.6}$$

In the following, we closely follow the proof of Theorem 1 in Ravikumar et al. (2009). The Lagrangian in (4) of the main manuscript, for fixed $\{\beta_j, j = 1, \dots, p\}$ can be rewritten as:

$$Q(\{g_j\}; \lambda) := \mathbb{E} \left[\left(\sum_{j=1}^p g_j^*(X_{\beta_j^*}, A) - \sum_{j=1}^p g_j(X_{\beta_j}, A) \right)^2 \right] + \lambda \sum_{j=1}^p \|g_j\|. \tag{S.7}$$

Fixing $\{\beta_j, j = 1, \dots, p\}$, for each j , let us consider the minimization of (S.7) with respect to the component function $g_j \in \mathcal{H}_j^{(\beta_j)}$, holding the other component functions $\{g_{j'}, j' \neq j\}$ fixed. The stationary condition is obtained by setting its Fréchet derivative to 0. Denote by $\partial_j Q(\{g_j\}; \lambda; \eta_j)$ the directional derivative with respect to $g_j \in \mathcal{H}_j^{(\beta_j)}$ ($j = 1, \dots, p$) in an arbitrary direction which we denote by $\eta_j \in \mathcal{H}_j^{(\beta_j)}$. Then, for fixed $\{\beta_j, j = 1, \dots, p\}$, the stationary point of the Lagrangian (S.7) can be formulated as:

$$\partial_j Q(\{g_j\}; \lambda; \eta_j) = 2\mathbb{E} \left[(g_j - \tilde{R}_j + \lambda \nu_j) \eta_j \right] = 0, \tag{S.8}$$

where

$$\tilde{R}_j := \sum_{j=1}^p g_j^*(X_{\beta_j^*}, A) - \sum_{j' \neq j} g_{j', A}(X_{\beta_{j'}}), \tag{S.9}$$

representing the partial residual for the j th component function g_j , and the function ν_j is an element of the subgradient $\partial \|g_j\|$, which satisfies $\nu_j = g_j / \|g_j\|$ if $\|g_j\| \neq 0$, and $\nu_j \in \{s \in \mathcal{H}_j^{(\beta_j)} \mid \|s\| \leq 1\}$, otherwise.

Applying the iterated expectations to condition on (X_{β_j}, A) , the stationary condition (S.8) can be rewritten as:

$$2\mathbb{E} \left[\left(g_j - \mathbb{E} \left[\tilde{R}_j | X_{\beta_j}, A \right] + \lambda \nu_j \right) \eta_j \right] = 0. \quad (\text{S.10})$$

Since the function $g_j - \mathbb{E} \left[\tilde{R}_j | X_{\beta_j}, A \right] + \lambda \nu_j \in \mathcal{H}_j^{(\beta_j)}$, we can evaluate (S.8) (i.e., expression (S.10)) in the particular direction: $\eta_j = g_j - \mathbb{E} \left[\tilde{R}_j | X_{\beta_j}, A \right] + \lambda \nu_j$, which gives $\mathbb{E} \left[\left(g_j - \mathbb{E} \left[\tilde{R}_j | X_{\beta_j}, A \right] + \lambda \nu_j \right)^2 \right] = 0$. This equation implies:

$$g_j + \lambda \nu_j = \mathbb{E} \left[\tilde{R}_j | X_{\beta_j}, A \right] \quad (\text{almost surely}). \quad (\text{S.11})$$

Let f_j denote the right-hand side of (S.11), i.e., $f_j (= f_j(X_{\beta_j}, A)) := \mathbb{E} \left[\tilde{R}_j | X_{\beta_j}, A \right]$. If $\|g_j\| \neq 0$, then $\nu_j = g_j / \|g_j\|$. Therefore, by (S.11), we have $\|f_j\| = \|g_j + \lambda g_j / \|g_j\|\| = \|g_j\| + \lambda \geq \lambda$. On the other hand, if $\|g_j\| = 0$, then $g_j = 0$ (almost surely), and $\|\nu_j\| \leq 1$. Then, condition (S.11) implies that $\|f_j\| \leq \lambda$. This gives us the equivalence between $\|f_j\| \leq \lambda$ and the statement $g_j = 0$ (almost surely). Therefore, condition (S.11) leads to the following expression:

$$(1 + \lambda / \|g_j\|) g_j = f_j \quad (\text{almost surely})$$

if $\|f_j\| > \lambda$, and $g_j = 0$ (almost surely), otherwise; this implies the soft thresholding update rule for g_j appeared in (5) of the main manuscript.

Now we will derive the expression (6) of the main manuscript for the function f_j . Note, the underlying model (S.1) (if we omit the components associated with the scalar covariates) implies that $\sum_{j=1}^p g_j^*(X_{\beta_j^*}, A) = \mathbb{E}[Y | \mathbf{X}, A] - \mu(\mathbf{X})$. Thus, (S.9) can be equivalently written as: $\tilde{R}_j = \mathbb{E}[Y | \mathbf{X}, A] - \mu(\mathbf{X}) - \sum_{j' \neq j} g_{j'}(X_{\beta_{j'}}, A)$. Therefore, the function $f_j(X_{\beta_j}, A) = \mathbb{E} \left[\tilde{R}_j | X_{\beta_j}, A \right]$ can be written as:

$$\begin{aligned} f_j(X_{\beta_j}, A) &= \mathbb{E} \left[\mathbb{E}[Y | \mathbf{X}, A] - \mu(\mathbf{X}) - \sum_{j' \neq j} g_{j'}(X_{\beta_{j'}}, A) \mid X_{\beta_j}, A \right] \\ &= \mathbb{E} \left[\mathbb{E}[Y | \mathbf{X}, A] - \sum_{j' \neq j} g_{j'}(X_{j'}, A) \mid X_{\beta_j}, A \right] - \mathbb{E}[\mu(\mathbf{X}) \mid X_{\beta_j}, A] \\ &= \mathbb{E} \left[Y - \sum_{j' \neq j} g_{j'}(X_{\beta_{j'}}, A) \mid X_{\beta_j}, A \right] - \mathbb{E}[\mu(\mathbf{X}) \mid X_{\beta_j}] \\ &= \mathbb{E} \left[Y - \sum_{j' \neq j} g_{j'}(X_{\beta_{j'}}, A) \mid X_{\beta_j}, A \right] - \mathbb{E} \left[\mu(\mathbf{X}) + \sum_{j=1}^p g_j^*(X_{\beta_j^*}, A) \mid X_{\beta_j} \right] \\ &= \mathbb{E} \left[Y - \sum_{j' \neq j} g_{j'}(X_{\beta_{j'}}, A) \mid X_{\beta_j}, A \right] - \mathbb{E}[Y \mid X_{\beta_j}] \\ &= \mathbb{E} \left[Y - \sum_{j' \neq j} g_{j'}(X_{\beta_{j'}}, A) \mid X_{\beta_j}, A \right] - \mathbb{E} \left[Y - \sum_{j' \neq j} g_{j'}(X_{\beta_{j'}}, A) \mid X_{\beta_j} \right] \\ &= \mathbb{E}[R_j \mid X_{\beta_j}, A] - \mathbb{E}[R_j \mid X_{\beta_j}], \end{aligned}$$

where the fourth equality of the expression follows from the identifiability constraint (S.2) of the underlying model (S.1), and the sixth equality follows from the optimization constraint $\mathbb{E}[g_{j'}(X_{\beta_{j'}}, A) | X_j] = 0$ ($j' \neq j$) implied by (S.4) imposed on $\{g_{j'}, j' \neq j\}$; this gives the expression (6) of the main manuscript for f_j .

A.3. Description of general linear smoothers for the component functions

As a remark to Section 3.2.1 of the main manuscript, we note that any scatterplot smoother can be utilized to obtain the sample counterpart (16) of the main manuscript of the coordinate-wise solution (5) for the component functions g_j , i.e., estimation of the component functions g_j is not restricted to regression splines.

To estimate the function f_j in (6), we can estimate the system of treatment a -specific functions $\mathbb{E}[R_j|\langle\widehat{\beta}_j, X_{ij}\rangle, A = a]$ ($a = 1, \dots, L$) (which corresponds to the first term on the right-hand side of (6) if we fix $\beta_j = \widehat{\beta}_j$), by performing separate nonparametric regressions of \widehat{R}_j on regressor $\langle\widehat{\beta}_j, X_{ij}\rangle$ separately for each treatment condition $A = a$ ($a = 1, \dots, L$). We can also estimate the function $-\mathbb{E}[R_j|\langle\beta_j, X_{ij}\rangle]$ (which corresponds to the second term $-\mathbb{E}[R_j|\langle\beta_j, X_{ij}\rangle]$ on the right-hand side of (6) if we fix $\beta_j = \widehat{\beta}_j$), by performing a nonparametric regression of \widehat{R}_j on regressor $\langle\widehat{\beta}_j, X_{ij}\rangle$. Adding these two function estimates provides an estimate for f_j in (6). Evaluating this estimate of f_j at the n points $(\langle\widehat{\beta}_j, X_{ij}\rangle, A_i)$ ($i = 1, \dots, n$) gives an estimate $\widehat{\mathbf{f}}_j \in \mathbb{R}^n$ in (16). Then we can compute the corresponding soft-threshold estimate $\widehat{\mathbf{g}}_j \in \mathbb{R}^n$ and conduct the coordinate descent procedure described in Algorithm 1 of the main manuscript.

A.4. Supplementary information for Section 3.2.1

The restriction of the function g_j to the form (12) of the main manuscript restricts also the minimizing function g_j in (5) of the main manuscript (note, $g_j(\langle X_j, \widehat{\beta}_j \rangle, A) = s_j^{(\lambda)} f_j(\langle X_j, \widehat{\beta}_j \rangle, A)$, where $s_j^{(\lambda)} = [1 - \lambda/\|f_j\|_+]_+$) to the form (12) of the main manuscript. In particular, we can express the function f_j in (6) of the main manuscript as:

$$\begin{aligned} f_{j,A}(\langle X_j, \widehat{\beta}_j \rangle) &= \mathbb{E}[R_j|\langle X_j, \widehat{\beta}_j \rangle, A] - \sum_{a=1}^L \pi_a \mathbb{E}[R_j|\langle X_j, \widehat{\beta}_j \rangle, A = a] \\ &= \Psi_j(\langle X_j, \widehat{\beta}_j \rangle) \boldsymbol{\theta}_{j,A}^* - \Psi_j(\langle X_j, \widehat{\beta}_j \rangle) \left\{ \sum_{a=1}^L \pi_a \boldsymbol{\theta}_{j,a}^* \right\}, \end{aligned} \quad (\text{S.12})$$

where $\{\boldsymbol{\theta}_{j,a}^*\}_{a \in \{1, \dots, L\}} := \underset{\{\boldsymbol{\theta}_{j,a} \in \mathbb{R}^{d_j}\}_{a \in \{1, \dots, L\}}}{\operatorname{argmin}} \mathbb{E} \left[\left\{ R_j - \Psi_j(\langle X_j, \widehat{\beta}_j \rangle)^\top \boldsymbol{\theta}_{j,A} \right\}^2 \right]$. In (S.12), the first term,

$\Psi_j(\langle X_j, \widehat{\beta}_j \rangle) \boldsymbol{\theta}_{j,A}^*$, corresponds to the L^2 projection of the j th partial residual R_j in (7) (of the main manuscript) onto the class of functions of the form (12) (without the imposition of the constraint (13), that is, the constraint $\sum_{a=1}^L \pi_a \boldsymbol{\theta}_{j,a} = \mathbf{0}$), whereas the second term, $-\Psi_j(\langle X_j, \widehat{\beta}_j \rangle) \left\{ \sum_{a=1}^L \pi_a \boldsymbol{\theta}_{j,a}^* \right\}$, simply centers the first term to satisfy the linear constraint, $\sum_{a=1}^L \pi_a \boldsymbol{\theta}_{j,a} = \mathbf{0}$. Then it follows that f_j , as given in (S.12), corresponds to the L^2 projection of R_j onto the subspace of measurable functions of the form (12) subject to the linear constraint (13) of the main manuscript.

A.5. Simulation results under a “linear” A -by- (\mathbf{X}, \mathbf{Z}) interaction effect scenario

In this subsection, as an extension of the simulation example in Section 4.1 of the main manuscript, we consider a case where the treatment effect varies *linearly* in the covariates (\mathbf{X}, \mathbf{Z}) , i.e., a “linear” A -by- (\mathbf{X}, \mathbf{Z}) interaction effect scenario and assess the ITR estimation performance of the methods. Specifically, we consider the data generation model:

$$\begin{aligned} Y_i &= \delta \left\{ \sum_{j=1}^8 \sin(\langle \eta_j, X_{ij} \rangle) + \sum_{k=1}^8 \sin(Z_{ik}) \right\} + \\ &4(A_i - 1.5) \left[\langle \beta_1, X_{i1} \rangle / 1.5 - \langle \beta_2, X_{i2} \rangle / 1.5 + Z_{i1} / 1.5 - Z_{i2} / 1.5 + \xi \{ \langle X_{i1}, X_{i2} \rangle / 1.5 + Z_{i1} Z_{i2} / 1.5 \} \right] + \epsilon_i, \end{aligned} \quad (\text{S.13})$$

in which, when $\xi = 0$, a functional *linear* model specifies the A -by- (\mathbf{X}, \mathbf{Z}) interaction effect term (i.e., the second term on the right-hand side of (S.13)). However, when $\xi = 1$, the underlying model (S.13) deviates from the exact linear A -by- (\mathbf{X}, \mathbf{Z}) interaction effect structure, and in such a case, the model CFAM-lin (as well as CFAM) is misspecified. The contribution to the variance of Y from the main and the interaction effect terms in (S.13) was made similar to that of the data generating model (25) of Section 4.1 of the main manuscript.

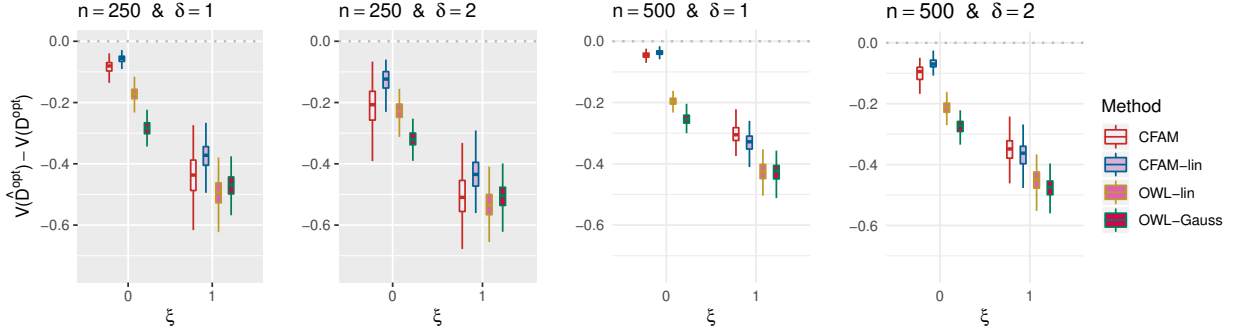


Figure S.1: Boxplots obtained from 200 Monte Carlo simulations comparing 4 approaches to estimating \mathcal{D}^{opt} , given each scenario indexed by $\xi \in \{0, 1\}$, $\delta \in \{1, 2\}$ and $n \in \{250, 500\}$. The dotted horizontal line represents the optimal value corresponding to \mathcal{D}^{opt} .

Figure S.1 illustrates the boxplots, obtained from 200 simulation runs, of the normalized values $V(\widehat{\mathcal{D}}^{opt}) - V(\mathcal{D}^{opt})$ (normalized by the optimal values $V(\mathcal{D}^{opt})$) of the decision rules $\widehat{\mathcal{D}}^{opt}$ estimated from the four approaches described in Section 4.1 of the main manuscript, for each combination of $n \in \{250, 500\}$, $\xi \in \{0, 1\}$ (corresponding to *correctly-specified* or *mis-specified* CFAM scenarios, respectively) and $\delta \in \{1, 2\}$ (corresponding to *moderate* or *large* main effects, respectively).

In all scenarios with $\xi = 0$ (i.e., when the linear interaction model is correctly specified), CFAM-lin outperforms CFAM, but by a relatively small amount in comparison to the difference in performance appearing in Figure 1 of the main manuscript, in which CFAM outperforms CFAM-lin. Moreover, if the underlying model deviates from the exact linear structure (i.e., $\xi = 1$ in model (S.13)) and $n = 500$, the more flexible CFAM tends to outperform CFAM-lin. Given the outstanding performance of CFAM compared to CFAM-lin in the *nonlinear A-by-(X, Z)* interaction effect scenarios considered in the main manuscript, this result suggests that, in the absence of prior knowledge about the form of the interaction effect, flexible modeling of the interaction effect using the proposed CFAM can lead to good results in comparison to CFAM-lin.

A.6. Separate modeling of the (\mathbf{X}, \mathbf{Z}) “main” effect component

Under model (S.1), constraint (S.2) (i.e., constraint (2) of the main manuscript) ensures that

$$E \left[\mu(\mathbf{X}, \mathbf{Z}) \left\{ \sum_{j=1}^p g_j(\langle X_j, \beta_j \rangle, A) + \sum_{k=1}^q h_k(Z_k, A) \right\} \right] = E \left[\mu(\mathbf{X}, \mathbf{Z}) E \left\{ \sum_{j=1}^p g_j(\langle X_j, \beta_j \rangle, A) + \sum_{k=1}^q h_k(Z_k, A) \mid \mathbf{X}, \mathbf{Z} \right\} \right] = 0,$$

where, on the right-hand side, we apply the iterated expectation rule to condition on (\mathbf{X}, \mathbf{Z}) , which implies:

$$\mu(\mathbf{X}, \mathbf{Z}) \perp \sum_{j=1}^p g_j(\langle X_j, \beta_j \rangle, A) + \sum_{k=1}^q h_k(Z_k, A) \quad (\text{S.14})$$

in L^2 . The orthogonality (S.14) conceptually and also practically implies that, under the squared error minimization criterion, the optimization for μ and the components $\{g_j, \beta_j, h_k\}$ in model (S.1) (subject to (S.2)) can be performed separately, without iterating between the two optimization procedures. To be specific, we can solve for the (\mathbf{X}, \mathbf{Z}) “main” effect:

$$\mu^* = \underset{\mu \in \mathcal{H}}{\operatorname{argmin}} E \left[\{Y - \mu(\mathbf{X}, \mathbf{Z})\}^2 \right], \quad (\text{S.15})$$

and can separately solve for the (\mathbf{X}, \mathbf{Z}) -by- A interaction effect via optimization (S.4). In optimization (S.15), \mathcal{H} represents a (possibly misspecified) L^2 space of functionals over (\mathbf{X}, \mathbf{Z}) . Even if the true μ in (S.1) is not

Table S.1: Comparison of the performance of CFAM and CFAM(μ), with respect to the parameter estimation assessed by the root squared error $\text{RSE}(\beta_j)$ (a smaller value of $\text{RSE}(\beta_j)$ is desired) and the optimal ITR estimation assessed by $V^*(\widehat{\mathcal{D}}^{opt}) = V(\widehat{\mathcal{D}}^{opt}) - V(\mathcal{D}^{opt})$ (a larger value of $V^*(\widehat{\mathcal{D}}^{opt})$ is desired), for varying $\delta \in \{1, 2\}$ and $n \in \{250, 500, 1000\}$.

		$\delta = 1$ (<i>Moderate</i> “main” effect)			$\delta = 2$ (<i>Large</i> “main” effect)		
		$n = 250$	$n = 500$	$n = 1000$	$n = 250$	$n = 500$	$n = 1000$
CFAM	$\text{RSE}(\beta_1)$	0.53(0.08)	0.34(0.02)	0.26(0.02)	0.60(0.14)	0.38(0.05)	0.29(0.03)
	$\text{RSE}(\beta_2)$	0.53(0.06)	0.34(0.02)	0.27(0.01)	0.59(0.13)	0.39(0.07)	0.29(0.03)
	$V^*(\widehat{\mathcal{D}}^{opt})$	-0.07(0.04)	-0.03(0.01)	-0.01(0.01)	-0.16(0.07)	-0.07(0.02)	-0.04(0.01)
CFAM(μ)	$\text{RSE}(\beta_1)$	0.52(0.06)	0.33(0.02)	0.26(0.01)	0.57(0.13)	0.36(0.03)	0.28(0.02)
	$\text{RSE}(\beta_2)$	0.52(0.06)	0.33(0.01)	0.26(0.01)	0.56(0.11)	0.36(0.04)	0.28(0.02)
	$V^*(\widehat{\mathcal{D}}^{opt})$	-0.06(0.04)	-0.02(0.01)	-0.01(0.00)	-0.12(0.05)	-0.05(0.01)	-0.02(0.01)

in the class \mathcal{H} , the representation (S.4) that specifies the optimal (\mathbf{X}, \mathbf{Z}) -by- A interaction effect components, i.e., $\{g_j^*, \beta_j^*, h_k^*\}$, is not affected by the possible misspecification for μ , due to the orthogonality (S.14).

For the case of a continuous outcome Y , Tian et al. (2014) (in the linear regression context with scalar covariates and Lasso regularization) and Park et al. (2020a) (in the single-index regression context with scalar covariates) proposed to separately model and fit the main effect component μ^* , by leveraging the orthogonality property analogous to (S.14), and then utilize the residualized outcome $Y - \widehat{\mu}^*(\mathbf{X}, \mathbf{Z})$ (instead of using the original outcome Y) for the estimation of the interaction effect components. This residualization procedure that utilizes separately fitted main effect was termed *efficiency augmentation* by Tian et al. (2014), and can improve the efficiency of the estimator for the interaction effect components (while maintaining the consistency of the estimator). In what follows, we illustrate an additional set of simulations supplementing the results of Section 4.1 of the main manuscript, which demonstrates some performance improvement of the CFAM method via an efficiency augmentation procedure.

Under the simulation model (25) of the main manuscript (in which the corresponding results are reported in Table 1 of the main manuscript) for generating the data, we report additional simulation results associated with the CFAM method when the (\mathbf{X}, \mathbf{Z}) “main” effect component of the data generating model (25) is modeled by a functional additive regression, i.e., by the model: $\mu(\mathbf{X}, \mathbf{Z}) = \sum_{j=1}^p \tilde{g}_j(\langle X_j, \tilde{\beta}_j \rangle) + \sum_{k=1}^q \tilde{h}_k(Z_k)$, estimated based on an L^1 regularization that is similar to (4) of the main manuscript, with the associated tuning parameters selected as in the CFAM method) and the corresponding residualized outcome is used to implement the CFAM method.

In Table S.1, those rows with the label “CFAM” correspond to what are reported in Table 1 of the main manuscript, whereas those with “CFAM(μ)” correspond to the cases where that “main” effect component μ is modeled by the functional additive regression model described above. As in Table 1 of the main manuscript, we report the root squared error $\text{RSE}(\beta_j) = \sqrt{\int (\widehat{\beta}_j(s) - \beta_j(s))^2 ds}$ ($j = 1, 2$), where the parameters β_1 and β_2 are given in the data model (25) of the main manuscript, and $\widehat{\beta}_1$ and $\widehat{\beta}_2$ are the corresponding estimates. In addition to RSE, we also report the optimal ITR estimation performance of CFAM and CFAM(μ), in terms of the (normalized) value $V^*(\widehat{\mathcal{D}}^{opt}) = V(\widehat{\mathcal{D}}^{opt}) - V(\mathcal{D}^{opt})$ (where a larger value of $V^*(\widehat{\mathcal{D}}^{opt})$ is desired).

The results in Table S.1 indicate that, especially when $\delta = 2$ (i.e, for the large “main” effect cases), the efficiency augmentation procedure based on the functional additive regression model for the (\mathbf{X}, \mathbf{Z}) “main” effect improves CFAM (comparing the rows that are labeled as CFAM vs. those of CFAM(μ)), in terms of both the parameter estimation performance, i.e., $\text{RSE}(\beta_j)$ ($j = 1, 2$) and the optimal ITR estimation performance, i.e., $V^*(\widehat{\mathcal{D}}^{opt})$.